

Deep Face Recognition: A Survey

Mei Wang, Weihong Deng

School of Information and Communication Engineering,
Beijing University of Posts and Telecommunications, Beijing, China.

wm0245@126.com, whdeng@bupt.edu.cn

Abstract—Driven by graphics processing units (GPUs), massive amounts of annotated data and more advanced algorithms, deep learning has recently taken the computer vision community by storm and has benefited real-world applications, including face recognition (FR). Deep FR methods leverage deep networks to learn more discriminative representations, significantly improving the state of the art and surpassing human performance (97.53%). In this paper, we provide a comprehensive survey of deep FR methods, including data, algorithms and scenes. First, we summarize the commonly used datasets for training and testing. Then, the data preprocessing methods are categorized into two classes: “one-to-many augmentation” and “many-to-one normalization”. Second, for algorithms, we summarize different network architectures and loss functions used in the state-of-the-art methods. Third, we review several scenes in deep FR, such as video FR, 3D FR and cross-age FR. Finally, some potential deficiencies of the current methods and several future directions are highlighted.

I. INTRODUCTION

Due to its nonintrusive and natural characteristics, face recognition (FR) has been the prominent biometric technique for identity authentication and has been widely used in many areas, such as military, finance, public security and daily life. FR has been a long-standing research topic in the CVPR community. In the early 1990s, the study of FR became popular following the introduction of the historical Eigenface approach [155]. The milestones of feature-based FR over the past years are presented in Fig. 1, in which the times of four major technical streams are highlighted. The holistic approaches derive the low-dimensional representation through certain distribution assumptions, such as linear subspace [10][107][41], manifold [64][186][40], and sparse representation [172][202][37][39]. This idea dominated the FR community in the 1990s and 2000s. However, a well-known problem is that these theoretically plausible holistic methods fail to address the uncontrolled facial changes that deviate from their prior assumptions. In the early 2000s, this problem gave rise to local-feature-based FR. Gabor [95] and LBP [4], as well as their multilevel and high-dimensional extensions [203][23][38], achieved robust performance through some invariant properties of local filtering. Unfortunately, handcrafted features suffered from a lack of distinctiveness and compactness. In the early 2010s, learning-based local descriptors were introduced to the FR community [18][86][19], in which local filters are learned for better distinctiveness, and the encoding codebook is learned for better compactness. However, these shallow representations still have an inevitable limitation on robustness against the complex nonlinear facial appearance variations.

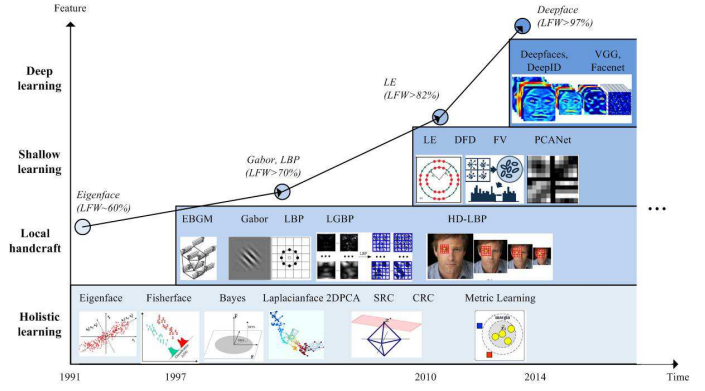


Fig. 1. Milestones of feature representation for face recognition.

In 2014, DeepFace [151] and DeepID [143] achieved state-of-the-art verification accuracy in LFW, surpassing human performance in the unconstrained scenario for the first time. Since then, research focus has shifted to deep-learning-based approaches that achieve transcendental feature invariance progressively through the stacking of nonlinear filters. Existing deep network architectures include convolutional neural networks (CNNs) [85], [140], [149], [61], deep belief networks (DBNs) [65], and stacked autoencoders (SAEs) [157]. Simulating the perception of the human brain, deep networks can represent high-level abstractions by multiple layers of nonlinear transformations. FR is slightly different from other object classification tasks because of the particularity of faces. First, numerous face images of large amounts of people make obtaining all the classes for training impractical. Second, intra-personal variations could be larger than inter-personal differences due to different poses, illuminations, expressions, ages, and occlusions. Therefore, deep neural networks have been not only introduced but also adjusted for FR from two aspects. One is from the data aspect, for which larger face databases are collected and images are preprocessed to improve learning ability. The other is from the algorithm aspect, for which novel architectures and loss functions are designed to promote the discrimination and generalization capability.

With the rapid developments in GPU hardware, big data and novel algorithms, deep FR techniques have fostered numerous startups with practical applications in recent five years. Over the past few years, there have been several surveys on FR [212], [15], [2], [75], [134] and its subdomains, including illumination-invariant FR [222], 3D FR [134], pose-invariant FR [206] and so on. However, the aforementioned surveys mainly cover the methodologies on shallow FR. In this survey,

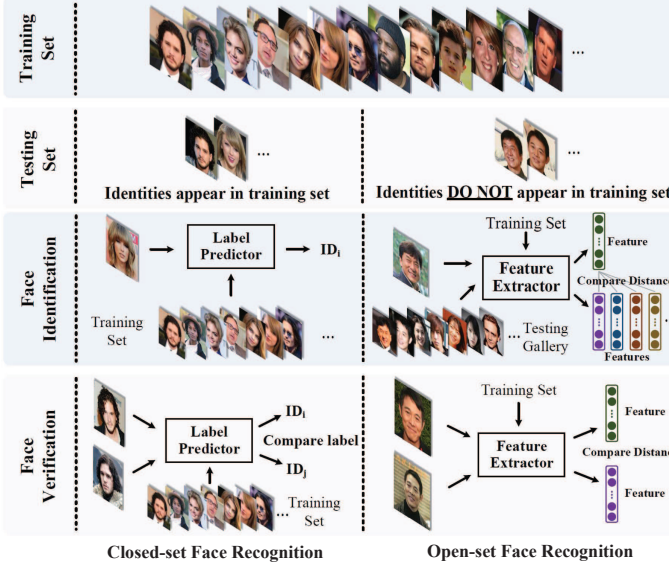


Fig. 2. Comparison of open-set and closed-set FR. [97]

we focus on up-to-date deep-feature-learning-based FR, as well as its closely related database development, data preprocessing, and feature classification methods. Face detection and alignment are beyond our consideration, and one can refer to Ranjan et al. [121], who provided a brief review of a full deep FR pipeline. Specifically, the key contributions of this survey are as follows:

- For data, some commonly used FR datasets are summarized. Moreover, the data preprocessing methods, which are used to handle intra-personal variations, particularly those caused by poses, are introduced and categorized into two classes: “one-to-many augmentation” and “many-to-one normalization”.
- For algorithms, some typical [85], [140], [149], [61] and novel network architectures used in deep FR are presented. Additionally, different loss functions are studied and categorized into Euclidean-distance-based loss, angular/cosine-margin-based loss and softmax loss and its variations.
- We review a dozen specific FR scenes that are still challenging for deep feature learning, such as anti-spoofing, cross-pose FR, and cross-age FR. These scenes reveal the important issues for future research on deep FR.

The remainder of this survey is structured as follows. In Section II, we introduce some background concepts and terminology, and then we briefly introduce each component of FR. In Section III, we summarize the datasets and the algorithms for data preprocessing. Then, different network architectures and loss functions are presented. In Section V, we briefly introduce several scenes of deep FR. Finally, the conclusion of this paper and discussion of future works are presented in Section VI.

II. OVERVIEW

A. Background Concepts and Terminology

As mentioned in [121], there are three modules needed for the whole system, as shown in Fig. 3. First, a face detector is used to localize faces in images or videos. Second, with the facial landmark detector, the faces are aligned to normalized canonical coordinates. Third, the FR module is implemented with these aligned face images. We only focus on the FR module throughout the remainder of this paper.

Furthermore, FR can be categorized as face verification and face identification. In either scenario, a set of known subjects is initially enrolled in the system (the gallery), and during testing, a new subject (the probe) is presented. Face verification computes one-to-one similarity between the gallery and probe to determine whether the two images are of the same subject, whereas face identification computes one-to-many similarity to determine the specific identity of a probe face. When the probe appears in the gallery identities, this is referred to as closed-set identification; when the probes include those who are not in the gallery, this is open-set identification.

B. Components of Face Recognition

Before a face image is fed to an FR module, face anti-spoofing, which recognizes whether the face is live or spoofed, can avoid different types of attacks. We treat it as one of the FR scenes and present it in Section IV-D2. Then, recognition can be performed. As shown in Fig. 3(c), an FR module consists of data preprocessing, deep feature extraction and similarity comparison, and it can be described as follows:

$$M[F(P_i(I_i)), F(P_j(I_j))] \quad (1)$$

where I_i and I_j are two face images, respectively; P stands for data preprocessing to handle intra-personal variations, such as poses, illuminations, expressions and occlusions; F denotes feature extraction, which encodes the identity information; and M means a face matching algorithm used to compute similarity scores.

1) *Data Preprocessing*: Although deep-learning-based approaches have been widely used due to their powerful representation, Ghazi et al. [49] proved that various conditions, such as poses, illuminations, expressions and occlusions, still affect the performance of deep FR and that data preprocessing is beneficial, particularly for poses. Since pose variation is widely regarded as a major challenge in automatic FR applications, we mainly summarize the deep methods of data preprocessing for poses in this paper. Other variations can be solved by similar methods.

The data preprocessing methods are categorized as “one-to-many augmentation” and “many-to-one normalization”, as shown in Table I.

- “One-to-many augmentation”: generating many images of the pose variability from a single image to enable deep networks to learn pose-invariant representations.
- “Many-to-one normalization”: recovering the canonical view of face images from one or many images of a nonfrontal view; then, FR can be performed as if it were under controlled conditions.

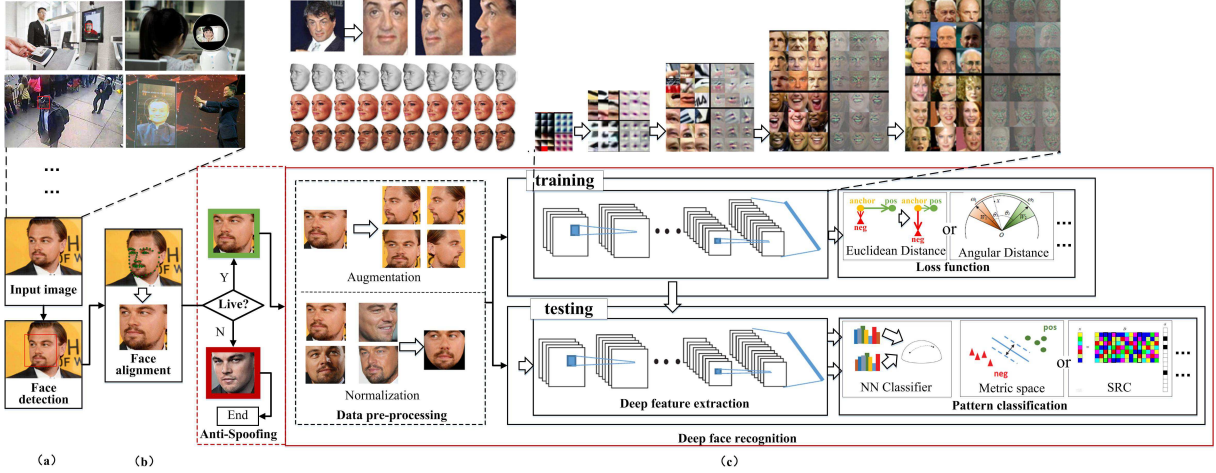


Fig. 3. Deep FR system with face detector and alignment.

TABLE I
DIFFERENT DATA PREPROCESSING APPROACHES

Data Preprocessing	Brief Description	Subsettings
one to many	generating many images of the pose variability from a single image	3D model [105], [103], [127], [128], [45] [54], [153], [152]
		2D deep model [220], [211], [139]
		data augmentation [96], [217], [43] [173], [143], [144], [148], [158]
		SAE [77], [208], [189]
many to one	recovering the canonical view of face images from one or many images of nonfrontal view	CNN [219], [221], [70], [32], [194]
		GAN [72], [154], [34], [197]

2) **Deep Feature Extraction: Network Architecture.** The architectures can be categorized as single and multiple networks, as shown in Table II. Inspired by the extraordinary success on the ImageNet [129] challenge, the typical CNN architectures, such as AlexNet, VGGNet, GoogleNet, and ResNet [85], [140], [149], [61], are introduced and widely used as the baseline model in FR (directly or slightly modified). In addition to the mainstream, there are still some novel architectures designed for FR to improve efficiency. Moreover, when adopting single networks as basic blocks, FR methods often train multiple networks with multiple inputs or multiple tasks. One network is for one type of input or one type of task. Hu et al. [68] shows that it provides an increase in performance after accumulating the results of multiple networks.

Loss Function. The softmax loss is commonly used as the supervision signal in object recognition, and it encourages the separability of features. However, for FR, when intra-variations could be larger than inter-differences, the softmax loss is not sufficiently effective for FR. Many works focus on creating novel loss functions to make features not only more separable but also discriminative, as shown in Table III.

- Euclidean-distance-based loss: compressing intra-variance and enlarging inter-variance based on Euclidean distance.
- angular/cosine-margin-based loss: learning discriminative face features in terms of angular similarity, leading to potentially larger angular/cosine separability between

learned features.

- softmax loss and its variations: directly using softmax loss or modifying it to improve performance, e.g., L2 normalization on features or weights as well as noise injection.

3) **Similarity Comparison:** After the deep networks are trained with massive data and an appropriate loss function, each of the test images is passed through the networks to obtain a deep feature representation. Once the deep features are extracted, most methods directly calculate the similarity between two features using cosine distance or L2 distance; then, the nearest neighbor (NN) and threshold comparison are used for both identification and verification tasks. In addition to these, other shallow methods are introduced to postprocess the deep features and perform the similarity comparison efficiently and accurately, such as metric learning, sparse-representation-based classifier (SRC), and so forth.

III. DEEP FACE RECOGNITION

A. Databases of Face Recognition

Zhou et al. [217] suggested that large amounts of data with deep learning improve the performance of FR, as shown in Fig. 4. Therefore, collecting a large dataset has always been a matter of concern.

In 2007, the LFW [71] was released to stimulate research in FR, specifically under unconstrained conditions. It contains 13,233 images (most of the faces are frontal) of 5749

TABLE II
DIFFERENT NETWORK ARCHITECTURES OF FR

Network Architectures	Subsettings
single network	typical architectures: AlexNet [131], [130], [135], VGGNet [115], [105], [205], GoogleNet [190], [135], ResNet [97], [205]
	novel architectures [175], [176], [148], [31], [182]
multiple networks	multipose [79], [104], [196], [165], multipatch [96], [217], [43], [146], [147], [143], [173], multitask [122]

TABLE III
DIFFERENT LOSS FUNCTIONS FOR FR

Loss Functions	Brief Description
Euclidean-distance-based loss	compressing intra-variance and enlarging inter-variance based on Euclidean distance. [143], [173], [144], [170], [179], [205], [135], [115], [131], [130], [96], [25]
angular/cosine-margin-based loss	making learned features potentially separable with larger angular/cosine distance. [98], [97], [160], [35], [162], [99]
softmax loss and its variations	modifying the softmax loss to improve performance. [120], [161], [57], [101] [119], [20], [58]

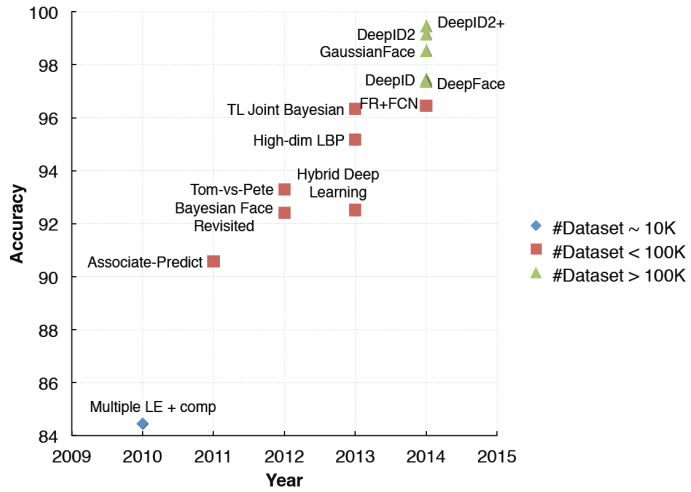


Fig. 4. The performances of different methods on the LFW. [217]

unique individuals, and it has six different standard evaluation protocols. Most deep learning methods follow the protocol defined for the “unrestricted, labeled outside data” setting. Since then, a wide variety of deep methods have worked with this database, and the performance approaches nearly 100%. Therefore, massive datasets are introduced to study the more difficult challenges, such as larger pose/age variations, larger distractors and low-shot learning. Here, we briefly introduce some important databases.

MS-Celeb-1M [56] is currently the largest public FR dataset, containing approximately 10M images of the 10K top celebrities from the 1 million celebrity list and linking to the unique entity keys in a knowledge base. In addition to recognizing large-scale faces, MS-Celeb-1M also provides 20,000 persons in a base set and 1,000 persons in a novel set for low-shot learning, where each person only has 1-5 images in the novel set. MS-Celeb-1M has some different characteristics from other databases. One is that there are overlaps between the identities of training set and test set. The other is that it chooses Precision and Coverage as its evaluation

metric to match with real scenarios in stead of using Rank-N or Accuracy. However, without manual filtering, there is label noise in MS-Celeb-1M. [35] decreases the noise of MS-Celeb-1M, and makes the refined dataset public available.

MegaFace [80], [108] includes 4.7M photos of 670K different individuals as the training set and increases the numbers of distractors to 1 million in the gallery set. However, an average of only 7 images per identity places restrictions on its intra-person variation, and it uses the subsets of FaceScrub [109] and FG-NET [112] to study the effects of pose and age variations.

IJB-A [84] contains 5,397 images and 2,042 videos of 500 subjects, which are split into 20,412 frames, 11.4 images and 4.2 videos per subject. It is a joint face detection and FR dataset, in which both face detection and facial feature point detection are accomplished manually. The key characteristics of IJB-A are that it contains a mixture of images and videos in the wild and covers a full range of pose variations.

CPLFW [213], SLLFW [42] and CALFW [215] are three datasets constructed for cross-pose, fine-grained and cross-age FR extended from LFW. CPLFW and CALFW search face pairs with large pose and age gaps using identities in LFW to form 3000 positive pairs, and negative pairs with the same gender and race are also selected to reduce the influence of attribute differences. The SLLFW replaces the 3000 negative pairs of LFW with 3000 similar-looking face pairs. As derivatives of LFW, the three small-scale datasets are light and ideal for performance evaluation due to the simple verification protocol but challenging face pairs.

There are many other publicly available FR datasets that have different characteristics and are designed for different FR scenes, as shown in Table IV. Apart from these public datasets, some Internet giants have access to a large collection of photos, and they build their own databases that are private to the public, such as Google [135] and Facebook [151].

When going deep into some large databases (photos > 1M), we can find some interesting conclusions about their training sets, as shown in Fig. 5. One is that these large training sets are expanded from depth or breadth. The deep datasets have

TABLE IV
THE COMMONLY USED FR DATASETS

Datasets	Publish Time	#photos	#subjects	# of photos per subject ¹	Metrics	Typical Methods & Accuracy ²	Key Features (Section)
LFW [71]	2007	13K	5K	1/2.3/550	1:1: Acc, TAR vs. FAR (ROC); 1:N: Rank-N, DIR vs. FAR (CMC)	99.78% Acc [120]; 99.63% Acc [135]	annotation with several attribute
MS-Celeb-1M [56]	2016	10M 3.8M(clean)	100,000 85K(clean)	100	Challenge-1: Coverage@P=0.95; Challenge-2: Coverage@P=0.99	Challenge-1: 79.10% @ P=0.95 [184]; Challenge-2: 99.01% @ P=0.99 [27]	large-scale; low-shot learning (IV-C1)
MegaFace [80], [108]	2016	4.7M	672,057	3/7/2469	1:1: TAR vs. FAR (ROC); 1:N: Rank-N (CMC)	1:1: 86.47% @ 10 ⁻⁶ FAR [135]; 1:N: 70.50% Rank-1 [135]	large-scale; 1 million distractors
IBB-A [84]	2015	25,809	500	11.4	1:1: TAR vs. FAR (ROC); 1:N: Rank-N, TPIR vs. FPIR (CMC, DET)	1:1: 92.10% @ 10 ⁻³ FAR [17]; 1:N: 98.20% Rank-1 [17]	cross-pose; template-based (IV-A1 and IV-C2)
CPLFW [213]	2017	11652	3968	2/2.9/3	1:1: Acc, TAR vs. FAR (ROC)	77.90% Acc [115]	cross-pose (IV-A1)
CFP [136]	2016	7,000	500	14	1:1: Acc, EER, AUC, TAR vs. FAR (ROC)	Frontal-Frontal: 98.67% Acc [117]; Frontal-Profile: 94.39% Acc [196]	frontal profile (IV-A1)
SLLFW [42]	2017	13K	5K	2.3	1:1: Acc, TAR vs. FAR (ROC)	85.78% Acc [115]; 78.78% Acc [151]	fine-grained
UMDFaces [9]	2016	367,920	8,501	43.3	1:1: Acc, TPR vs. FPR (ROC)	69.30% @ 10 ⁻² FAR [85]	annotation with bounding boxes, 21 keypoints, gender and 3D pose
YTF [171]	2011	3,425	1,595	48/181,3/6,070	1:1: Acc	97.30% Acc [115]; 96.52% Acc [124]	video (IV-C3)
PasC [11]	2013	2,802	265	—	1:1: VR vs. FAR (ROC)	95.67% @ 10 ⁻² FAR [124]	video (IV-C3)
YTC [82]	2008	1,910	47	—	1:N: Rank-N (CMC)	97.82% Rank-1 [124]; 97.32% Rank-1 [123]	video (IV-C3)
CALFW [215]	2017	12174	4025	2/3/4	1:1: Acc, TAR vs. FAR (ROC)	86.50% Acc [115]; 82.52% Acc [20]	cross-age; 12 to 81 years old (IV-A2)
MORPH [126]	2006	55,134	13,618	4.1	1:N: Rank-N (CMC)	94.4% Rank-1 [93]	cross-age, 16 to 77 years old (IV-A2)
CACD [21]	2014	163,446	2000	81.7	1:1 (CACD-VS): Acc, TAR vs. FAR (ROC) 1:N: MAP	1:1 (CACD-VS): 98.50% Acc [169] 1:N: 69.96% MAP (2004+2006)[214]	cross-age, 14 to 62 years old (IV-A2)
FG-NET [1]	2010	1,002	82	12.2	1:N: Rank-N (CMC)	88.1% Rank-1 [169]	cross-age, 0 to 69 years old (IV-A2)
CASIA NIR-VIS v2.0 [89]	2013	17,580	725	24.2	1:1: Acc, VR vs. FAR (ROC)	98.62% Acc, 98.32% @ 10 ⁻³ FAR [177]	NIR-VIS; with eyeglasses, pose and expression variation (IV-B1)
CASIA-HFB [90]	2009	5097	202	25.5	1:1: Acc, VR vs. FAR (ROC)	97.58% Acc, 85.00% @ 10 ⁻³ FAR [125]	NIR-VIS; with eyeglasses and expression variation (IV-B1)
CUFS [166]	2009	1,212	606	2	1:N: Rank-N (CMC)	100% Rank-1 [201]	sketch-photo; lighting variation;
CUFSF [204]	2011	2,388	1,194	2	1:N: Rank-N (CMC)	51.00% Rank-1 [163]	shape exaggeration (IV-B3)
Bosphorus [132]	2008	4,652	105	31/44,3/54	1:1: TAR vs. FAR (ROC); 1:N: Rank-N (CMC)	1:N: 99.20% Rank-1 [81]	3D; 34 expressions, 4 occlusions and different poses (IV-D1)
BU-3DFE [195]	2006	2,500	100	25	1:1: TAR vs. FAR (ROC); 1:N: Rank-N (CMC)	1:N: 95.00% Rank-1 [81]	3D; different expressions (IV-D1)
FRGCv2 [118]	2005	4,007	466	1/8,6/22	1:1: TAR vs. FAR (ROC); 1:N: Rank-N (CMC)	1:N: 94.80% Rank-1 [81]	3D; different expressions (IV-D1)
Guo et al. [52]	2014	1,002	501	2	1:1: Acc, TAR vs. FAR (ROC)	94.8% Rank-1, 65.9% @ 10 ⁻³ FAR [91]	make-up; female (IV-A3)
FAM [69]	2013	1,038	519	2	1:1: Acc, TAR vs. FAR (ROC)	88.1% Rank-1, 52.6% @ 10 ⁻³ FAR [91]	make-up; female and male (IV-A3)
CASIA-FASD [209]	2012	600	50	12	EER, HTER	2.67% EER, 2.27% HTER [7]	anti-spoofing (IV-D2)
Replay-Attack [28]	2012	1300	50	—	EER, HTER	0.79% EER, 0.72% HTER [7]	anti-spoofing (IV-D2)
CASIA WebFace [192]	2014	494,414	10,575	2/46,8/804	— (mainly used for training)	—	
CelebFaces+ [143]	2014	202,599	10,177	19.9	— (mainly used for training)	—	
UMDFaces-Videos [8]	2017	22,075	3,107	—	— (mainly used for training)	—	
VGGFace2 [17]	2017	3.31M	9,131	87/362,6/843	— (mainly used for training)	—	
VGGFace [115]	2015	2.6M	2,622	1,000	— (mainly used for training)	—	
Google [135]	2015	>500M	>10M	50	— (mainly used for training)	—	
Facebook [151]	2014	4.4M	4K	80/1100/1200	— (mainly used for training)	—	private

¹ The min/average/max numbers of photos or frames per subject

² We only present the typical methods that are published in a paper, and the accuracies of the most challenging scenarios are given.

limited number of subjects but many images for each subjects, such as VGGface and VGGface2; contrarily, breadth means many subject but limited images for each subjects, such as Megaface (an average of 7 images per identity). Depth enables deep models to handle variation while breadth increases the possibility of overlaps between training set and test set. The other is that the utilization of long tail distribution is different among datasets. For example, in challenge2 of MS-Celeb-1M, the novel set specially uses the tailed data to study low-shot learning, while the base set uses the central part of the distribution and limits the number of images to 50-100 per person to ensure general facial perceptions of models; the central part is also used by the challenge1 of MS-Celeb-1M and images' number is approximately 100 for each celebrity; VGGface and VGGface2 only use the head part to construct deep databases; Megaface utilizes the whole distribution to contain as many images as possible, the minimal number of images is 3 per person and the maximum is 2469.

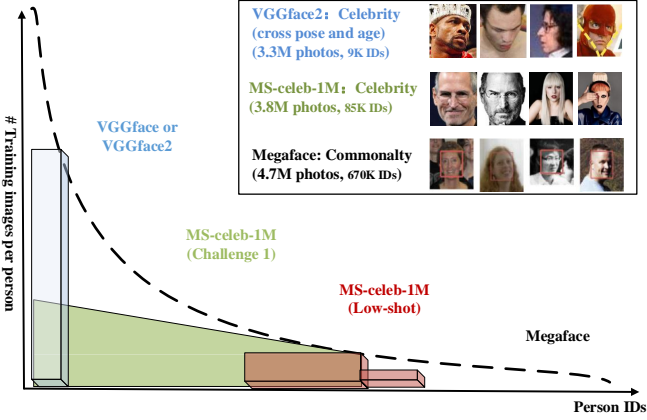


Fig. 5. The distribution of different large databases. The vertical axis displays number of images per person, and the horizontal axis shows person IDs.

B. Data Preprocessing Algorithms

1) *One-to-Many Augmentation*: Collecting a large database is extremely expensive and time consuming, and occasionally, it cannot enable deep networks to learn intra-class variations due to the long tail phenomenon [217]. The methods of “one-to-many augmentation” are used to mitigate the challenges of data collection, and they can be categorized into three classes: data augmentation, 3D model and 2D deep model.

Data augmentation. Common data augmentation methods consist of photometric transformations [140], [85] and geometric transformations, such as oversampling (multiple patches obtained by cropping at different scales) [85], mirroring [187], and rotating [180] the images. Recently, data augmentation has been widely used in deep FR algorithms [96], [217], [43], [173], [143], [144], [148], [158]. for example, Sun et al. [143] cropped 400 face patches varying in positions, scales, and color channels and mirrored the images. In [96], seven CNNs with the same structure were used on seven overlapped image patches centered at different landmarks on the face region.

3D model. 3D face reconstruction is also a way to enrich the diversity of training data. There is a large number of

papers about this domain, but we only focus on the 3D face reconstruction using deep methods or used for deep FR. In [105], Masi et al. generated face images with new intra-class facial appearance variations, including pose, shape and expression, and then trained a 19-layer VGGNet with both real and augmented data. [103] used generic 3D faces and rendered fixed views to reduce much of the computational effort. Richardson et al. [127] employed an iterative CNN by using a secondary input channel to represent the previous network’s output as an image for reconstructing a 3D face. Dou et al. [45] used a multi-task CNN to divide 3D face reconstruction into neutral 3D reconstruction and expressive 3D reconstruction. [153] directly regressed 3D morphable face model (3DMM) [13] parameters from an input photo by a very deep CNN architecture.

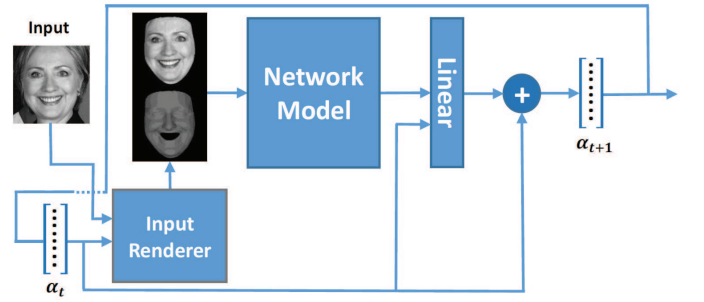


Fig. 6. Iterative CNN network for reconstructing a 3D face. [127]

2D deep model. Rather than reconstructing 3D models from a 2D image and projecting it back into 2D images of different poses, 2D deep models can generate 2D images directly. In the multi-view perceptron (MVP) [220], the deterministic hidden neurons learn the identity features, while the random hidden neurons capture the view features. By sampling different random neurons, the face images of different poses are synthesized. In [211], after using a 3D model to generate profile face images, Zhao et al. refined the images by a generative adversarial network (GAN) [50], which combines prior knowledge of the data distribution and knowledge of faces (pose and identity perception loss).

2) *Many-to-One Normalization*: In contrast to “one-to-many augmentation”, the methods of “many-to-one normalization” produce frontal faces and reduce appearance variability to make faces easy to align and compare. It can be categorized as SAE, CNN and GAN models.

SAE. The proposed stacked progressive autoencoders (SPAЕ) [77] progressively map the nonfrontal face to the frontal face through a stack of several autoencoders. In [189], a novel recurrent convolutional encoder-decoder network combined with shared identity units and recurrent pose units can render rotated objects instructed by control signals at each time step. Zhang et al. [208] built a sparse many-to-one encoder by setting frontal face and multiple random faces as the target values.

CNN. Zhu et al. [219] extracted face identity-preserving features to reconstruct face images in the canonical view using a CNN that consists of a feature extraction module and a frontal face reconstruction module. [221] selected canonical-

view images according to the face images' symmetry and sharpness and then adopted a CNN to recover the frontal view images by minimizing the reconstruction loss error. Yim et al. [194] proposed a multi-task network that can rotate an arbitrary pose and illumination image to the target-pose face image by utilizing the user's remote code. [70] transformed nonfrontal face images to frontal images according to the displacement field of the pixels between them.

GAN. [72] proposed a two-pathway generative adversarial network (TP-GAN) that contains four landmark-located patch networks and a global encoder-decoder network. Through combining adversarial loss, symmetry loss and identity-preserving loss, TP-GAN generates a frontal view and simultaneously preserves global structures and local details. In a disentangled representation learning generative adversarial network (DR-GAN) [154], an encoder produces an identity representation, and a decoder synthesizes a face at the specified pose using this representation and a pose code. [197] incorporated 3DMM into the GAN structure to provide shape and appearance priors to guide the generator to frontalization.

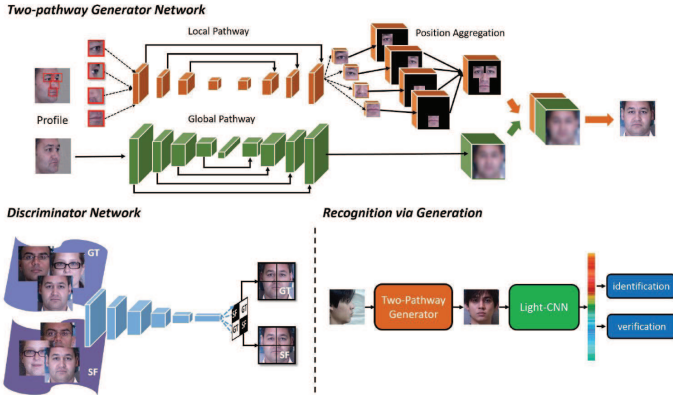


Fig. 7. General framework of TP-GAN. [72]

C. Categories of Network Architecture

1) **Single Network : Typical architectures.** The commonly used network architectures of deep FR have always followed those of deep object classification and evolved from AlexNet to ResNet rapidly. We present the most influential architectures that have shaped the current state-of-the-art of deep object classification and deep FR in chronological order¹ in Fig. 8.

In 2012, AlexNet [85] was reported to achieve state-of-the-art recognition accuracy in the ImageNet large-scale visual recognition competition (ILSVRC) 2012, exceeding the previous best results by a large margin. AlexNet consists of five convolutional layers and three fully connected layers, and it also integrates various techniques, such as rectified linear unit (ReLU), dropout, data augmentation, and so forth. ReLU was widely regarded as the most essential component for making deep learning possible. Then, in 2014, VGGNet [140] proposed a standard network architecture that used very small 3×3 convolutional filters throughout and doubled the number of feature maps after the 2×2 pooling. It increased the depth

of the network to 16-19 weight layers, which further enhanced the flexibility to learn progressive nonlinear mappings by deep architectures. In 2015, the 22-layer GoogleNet [149] introduced an “inception module” with the concatenation of hybrid feature maps, as well as two additional intermediate softmax supervised signals. It performs several convolutions with different receptive fields (1×1 , 3×3 and 5×5) in parallel, and it concatenates all feature maps to merge the multi-resolution information. In 2016, ResNet [61] proposed making layers learn a residual mapping with reference to the layer inputs $\mathcal{F}(x) := \mathcal{H}(x) - x$ rather than directly learning a desired underlying mapping $\mathcal{H}(x)$ to ease the training of very deep networks (up to 152 layers). The original mapping is recast into $\mathcal{F}(x) + x$ and can be realized by “shortcut connections”. With the evolved architectures and advanced training techniques, such as batch normalization (BN), the network becomes deeper and the training becomes more controllable, and the performance of object classification is continually improving.

Motivated by the substantial progress in object classification, the deep FR community follows these typical architectures step by step. In 2014, DeepFace [151] was the first to use a nine-layer CNN with several locally connected layers. With 3D alignment for data preprocessing, it reaches an accuracy of 97.35%. In 2015, FaceNet [135] used a large private dataset to train a GoogleNet. It adopted a triplet loss function based on triplets of roughly aligned matching/nonmatching face patches generated by a novel online triplet mining method and achieved good performance (99.63%). In the same year, VGGface [115] designed a procedure to collect a large-scale dataset from the Internet. It trained the VGGNet on this dataset and then fine-tuned the networks via a triplet loss function similar to FaceNet. VGGface obtains an accuracy of 98.95% on LFW. In 2017, SphereFace [97] used a 64-layer ResNet architecture and proposed the angular softmax (A-Softmax) loss to learn discriminative face features (SphereFace) with angular margin (99.42%).

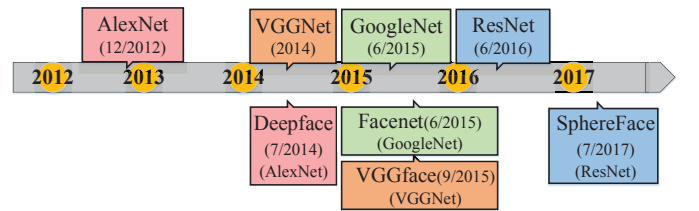


Fig. 8. The top row presents the typical network architectures in object classification, and the bottom row describes the well-known algorithms of deep FR that use the typical architectures and achieve good performance.

Novel architectures. In addition, there are some novel architectures in FR. [176], [175] proposed a max-feature-map (MFM) activation function that introduces the concept of maxout in the fully connected layer to CNN. The MFM obtains a compact representation and reduces the computational cost. Inspired by [94], Chowdhury et al. [31] applied the bilinear CNN (B-CNN) in FR. The outputs at each location of two CNNs are combined (using outer product) and are then average pooled to obtain the bilinear feature representation.

¹The time we present is when the paper was published.

[148] proposed sparsifying deep networks iteratively from the previously learned denser models based on a weight selection criterion. Conditional convolutional neural network (c-CNN) [182] dynamically activated sets of kernels according to modalities of samples. Although the light-weight CNNs for mobile devices, such as SqueezeNet, MobileNet, ShuffleNet and Xception [73], [67], [30], [207], are still not widely used in FR, they have potential and deserve more attention.

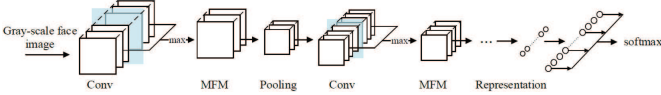


Fig. 9. The architecture of light CNN.

2) **Multiple Networks : Multi-input networks.** Corresponding to “one-to-many augmentation”, which generate multiple images of different patches or poses, the architectures also change into multiple networks for different image inputs. In [96], [217], [43], [146], [147], [143], [173], multiple networks are built after different numbers of face patches are cropped, and then one network handles one type of patch for representation extraction. [104], [79], [165] used multiple networks to handle images of different poses. For example, [104] adjusted the pose to frontal (0°), half-profile (40°) and full-profile views (75°) and then addressed pose variation by multiple pose networks. A multi-view deep network (MvDN) [79] consists of view-specific subnetworks and common subnetworks; the former removes view-specific variations, and the latter obtains common representations. Wang et al. [165] used coupled SAE for cross-view FR.

Multi-task learning networks. The other form of multiple networks is for multi-task learning, where identity classification is the main task, and the side tasks are pose, illumination, and expression estimations, among others. In these networks, the lower layers are shared among all the tasks, and the higher layers are disentangled into multiple networks to generate the task-specific outputs. In [122], the task-specific subnetworks are branched out to learn face detection, face alignment, pose estimation, gender recognition, smile detection, age estimation and FR. [196] proposed automatically assigning the dynamic loss weights for each side task. [117] used a feature reconstruction metric learning to disentangle a CNN into subnetworks for identity and pose.

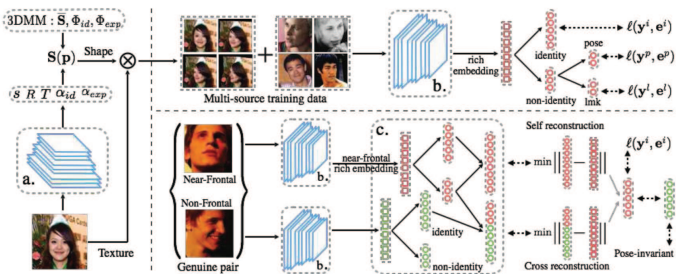


Fig. 10. Reconstruction-based disentanglement for pose-invariant FR. [117]

D. Methods of Loss Functions

1) **Euclidean-distance-based Loss :** Euclidean-distance-based loss is a metric learning [181], [168] that embeds images into Euclidean space and compresses intra-variance and enlarges inter-variance. The contrastive loss and the triplet loss are the commonly used loss functions. The contrastive loss [173], [143], [144], [148], [192] requires face image pairs and then pulls together positive pairs and pushes apart negative pairs. Sun et al. [173] combined the face identification and verification supervisory signals to learn a discriminative representation, and joint Bayesian (JB) was applied to obtain a robust embedding space. Extending from [173], [143] increased the dimension of hidden representations and added supervision to early convolutional layers, while [144] further introduced VGGNet and GoogleNet to their work. Triplet loss [135], [115], [130], [131], [96], [43] requires the face triplets, and then it minimizes the distance between an anchor and a positive sample of the same identity and maximizes the distance between the anchor and a negative sample of a different identity. [135] first introduced triplet loss to deep FR to make $\|f(x_i^a) - f(x_i^p)\|_2^2 + \alpha < \|f(x_i^a) - f(x_i^n)\|_2^2$ using hard triplet face samples, where x_i^a , x_i^p and x_i^n are the anchor, positive and negative samples, respectively; α is a margin; and $f(\cdot)$ represents a nonlinear transformation embedding an image into a feature space. Inspired by [135], [130], [131] learned a linear projection W to construct triplet loss, where the former satisfied Eq. 2 and the latter followed Eq. 3.

$$(x_i^a)^T W^T W x_i^p + \alpha < (x_i^a)^T W^T W x_i^n \quad (2)$$

$$(x_i^a - x_i^p)^T W^T W (x_i^a - x_i^p) + \alpha < (x_i^a - x_i^n)^T W^T W (x_i^a - x_i^n) \quad (3)$$

Other methods combine triplet loss with softmax loss [217], [96], [43], [33]. They first train networks with the softmax and then fine-tune them with triplet loss. However, the contrastive loss and triplet loss occasionally encounter training instability due to the selection of effective training samples.

An alternative is the center loss [170] and its variant [205], [36], [179]. In [170], the center loss learned a center for each class and penalized the distances between the deep features and their corresponding class centers. This loss can be defined as follows:

$$\mathcal{L}_C = \frac{1}{2} \sum_{i=1}^m \|x_i - c_{y_i}\|_2^2 \quad (4)$$

where x_i denotes the i th deep feature belonging to the y_i th class and c_{y_i} denotes the y_i th class center of deep features. To handle the long-tailed data, [205] used a range loss to minimize k greatest range’s harmonic mean values in one class and maximize the shortest inter-class distance within one batch, while [179] proposed a center-invariant loss that penalizes the difference between each center of classes. [36] selected the farthest intra-class samples and the nearest inter-class samples to compute a margin loss.

2) **Angular/cosine-margin-based Loss :** Angular/cosine-margin-based loss [98], [97], [160], [35], [99] makes learned features potentially separable with a larger angular/cosine distance. [98] reformulated the original softmax loss into a large-margin softmax (L-Softmax) loss, which requires

$\|W_1\| \|x\| \cos(m\theta_1) > \|W_2\| \|x\| \cos(\theta_2)$, where m is a positive integer introducing an angular margin, W is the weight of the last fully connected layer, x denotes the deep feature and θ is the angle between them. The loss function is defined as follows:

$$\mathcal{L}_i = -\log \left(\frac{e^{\|W_{y_i}\| \|x_i\| \varphi(\theta_{y_i})}}{e^{\|W_{y_i}\| \|x_i\| \varphi(\theta_{y_i})} + \sum_{j \neq y_i} e^{\|W_{y_i}\| \|x_i\| \cos(\theta_j)}} \right) \quad (5)$$

where

$$\varphi(\theta) = (-1)^k \cos(m\theta) - 2k, \theta \in \left[\frac{k\pi}{m}, \frac{(k+1)\pi}{m} \right] \quad (6)$$

Based on L-Softmax, A-Softmax loss [97] further normalized the weight W by its L2 norm ($\|W\| = 1$) such that the normalized vector will lie on a hypersphere, and then the discriminative face features can be learned on a hypersphere manifold with an angular margin. [99] introduced a deep hyperspherical convolution network (SphereNet) that adopts hyperspherical convolution as its basic convolution operator and is supervised by angular-margin-based loss. In contrast to L-Softmax and A-Softmax, which incorporate the angular margin in a multiplicative manner, [35] and [160], [162] respectively introduced an additive angular/cosine margin $\cos(\theta + m)$ and $\cos\theta - m$ for the softmax loss. The decision boundaries under the binary classification case are given in Table V.

TABLE V
DECISION BOUNDARIES FOR CLASS 1 UNDER BINARY CLASSIFICATION CASE, WHERE \hat{x} IS THE NORMALIZED FEATURE. [35]

Loss Functions	Decision Boundaries
Softmax	$(W_1 - W_2)x + b_1 - b_2 = 0$
L-Softmax [98]	$\ x\ (\ W_1\ \cos(m\theta_1) - \ W_2\ \cos(\theta_2)) > 0$
A-Softmax [97]	$\ x\ (\cos m\theta_1 - \cos \theta_2) = 0$
CosineFace [160]	$\hat{x} (\cos \theta_1 - m - \cos \theta_2) = 0$
ArcFace [35]	$\hat{x} (\cos(\theta_1 + m) - \cos \theta_2) = 0$

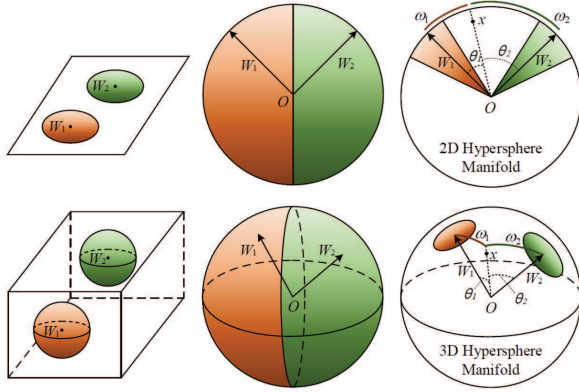


Fig. 11. Geometry interpretation of A-Softmax loss. [97]

3) *Softmax Loss and its Variations* : The softmax loss is a common choice for classification tasks, but it often has limitations in FR. In addition to reformulating softmax loss into an angular/cosine-margin-based loss as mentioned above, there are also many works focusing on modifying it in detail.

Normalization of feature or weight in softmax loss is one of the strategies, which can be written as follows:

$$\hat{W} = \frac{W}{\|W\|}, \hat{x} = \alpha \frac{x}{\|x\|} \quad (7)$$

where α is a scaling parameter. Scaling x to a fixed radius α is important, as [161] proved that normalizing the features and weights to 1 will make the softmax loss become trapped at a very high value on the training set.

In [97], [160], [35], [99], the loss functions normalized the weights only and trained with angular/cosine margin to make the learned features be discriminative. In contrast, some works, such as [120], [57], adopted feature normalization only to overcome the bias to the sample distribution of the softmax. Based on the observation of [114] that the L2-norm of features learned using the softmax loss is informative of the quality of the face, [120] enforced all the features to have the same L2-norm by feature normalization such that similar attention is given to good quality frontal faces and blurry faces with extreme pose. Rather than scaling parameter α , [57] normalized features with $\hat{x} = \frac{x - \mu}{\sqrt{\sigma^2}}$, where μ and σ^2 are the mean and variance. Moreover, normalizing both features and weights [161], [101], [58] has become a common strategy in softmax. In [161], Wang et al. explained the necessity of this normalization operation from both analytic and geometric perspectives. After normalizing features and weights, [101] optimized the cosine distance among data features, and [58] used the von Mises-Fisher (vMF) mixture model as the theoretical basis to develop a novel vMF mixture loss and its corresponding vMF deep features.

In addition to normalization, there are also other strategies to modify softmax; for example, [20] proposed a noisy softmax to mitigate early saturation by injecting annealed noise in softmax.

E. Similarity Comparison

During testing, the cosine distance and L2 distance are generally employed to measure the similarity between the deep features x_1 and x_2 ; then, threshold comparison and the nearest neighbor (NN) classifier are used for similarity comparison. Moreover, metric learning, which aims to find a new metric to make two classes more separable, can also be used for FR based on extracted deep features. The JB [22] model is a well-known metric learning method [173], [143], [144], [147], [192], and [68] proved that it can improve the performance greatly. In the JB model, a face feature x is modeled as $x = \mu + \varepsilon$, where μ and ε are identity and intra-personal variations, respectively. The similarity score $r(x_1, x_2)$ can be represented as follows:

$$r(x_1, x_2) = \log \frac{P(x_1, x_2 | H_I)}{P(x_1, x_2 | H_E)} \quad (8)$$

where $P(x_1, x_2 | H_I)$ is the probability that two faces belong to the same identity and $P(x_1, x_2 | H_E)$ is the probability that two faces belong to different identities.

In addition to these common methods, there are some other explorations. Based on deep features, [158] first used product quantization (PQ) [76] to directly retrieve the top-k

most similar faces and re-ranked these faces by combining similarities from deep features and the COTS matcher [51]. In [191], Yang et al. extracted the local adaptive convolution features from the local regions of the face image and used the extended SRC for FR with a single sample per person. [53] combined deep features and the SVM classifier to recognize all the classes.

F. Other Techniques for Deep Face Recognition

Transfer learning [111], [164] has recently been introduced for deep FR, which utilizes data in relevant source domains to execute FR in a target domain. [33], [183] adopted template adaptation, which is a form of transfer learning to the set of media in a template, by combining CNN features with template-specific linear SVMs. Kan et al. [78] proposed a bi-shifting autoencoder network (BAE) for domain adaptation across view angle, ethnicity, and imaging sensor. [141] used adversarial learning [156] to transfer knowledge of still image FR to video FR. Fine-tuning the CNN parameters from a prelearned model using a target training dataset is a particular form of transfer learning. It is commonly employed by numerous methods [3], [159], [25].

Recently, an end-to-end system [60], [174], [216], [26] was proposed to jointly train FR with several modules (face detection, alignment, and so forth) together. Compared to the existing methods in which each module is generally optimized separately according to different objectives, this end-to-end system optimizes each module according to the recognition objective, leading to more adequate and robust inputs for the recognition model. For example, inspired by spatial transformer [74], [60] proposed a CNN-based data-driven approach that learns to simultaneously register and represent faces, while [174] designed a novel recursive spatial transformer (ReST) module for CNN allowing face alignment and recognition to be jointly optimized.

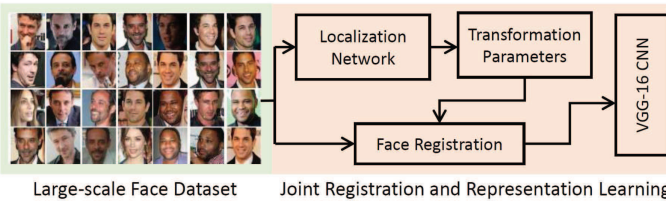


Fig. 12. Joint face registration and representation. [60]

IV. REAL-WORLD SCENES

In this section, we present some scenes of FR, as shown in Fig. 13. According to their characteristics, we divide these scenes into four categories: cross-factor FR, heterogenous FR, multiple (or single) media FR and FR in industry.

- Cross-factor FR. Due to the complex nonlinear facial appearance, some variations will be caused by people themselves, such as pose, age, make-up, expression and occlusion. In reality, the FR system should recognize person under these cross factors. The commonly used methods can be categorized into three settings: image

synthetic, domain adaptation and separating cross factors from identity.

- Heterogenous FR. It refers to the problem of matching faces across different visual domains. The domain gap is mainly caused by sensory devices and cameras settings, e.g. visual light vs. near-infrared. Domain adaptation and image synthetic are still effective methods to handle this problem.
- Multiple (or single) media FR. Ideally, deep models are trained with massive images per person and are tested with one image per person, but the situation will be different in reality. Sometimes, the number of images per person in training set could be very small, namely low-shot FR; or each subject face in test set is often enrolled with a set of images and videos, namely set-based FR.
- FR in industry. Although deep FR has achieved beyond human performance on some standard benchmarks, but some factors should be given more attention rather than accuracy when deep FR are adopted in industry, e.g. anti-spoofing and high efficiency.

A. Cross-Factor Face Recognition

1) *Cross-Pose Face Recognition*: As [136] shows that many existing algorithms suffer a decrease of over 10% from frontal-frontal to frontal-profile verification, cross-pose FR is still an extremely challenging scene. In addition to the aforementioned methods, including “one-to-many augmentation”, “many-to-one normalization”, multi-input networks and multi-task learning (Sections III-B and III-C2), there are still some other algorithms for cross-pose FR. Considering the extra burden of the above methods, [16] first attempt to perform frontalization in the deep feature space but not in the image space. A deep residual equivariant mapping (DREAM) block dynamically adds residuals to an input representation to transform a profile face to a frontal image. [24] proposed combining feature extraction with multi-view subspace learning to simultaneously make features be more pose robust and discriminative.

2) *Cross-Age Face Recognition*: Cross-age FR is extremely challenging due to the changes in facial appearance by the aging process over time. One direct approach is to synthesize the input image to the target age. A generative probabilistic model was used by [46] to model the facial aging process at each short-term stage. Antipov et al. [6] proposed aging faces by GAN, but the synthetic faces cannot be directly used for face verification due to its imperfect preservation of identities. Then, [5] used a local manifold adaptation (LMA) approach to solve the problem of [6]. An alternative is to decompose aging/identity components separately and extract age-invariant representations. [169] developed a latent identity analysis (LIA) layer to separate the two components. In [214], age-invariant features were obtained by subtracting age-specific factors from the representations with the help of the age estimation task. Additionally, there are other methods for cross-age FR. For example, [12], [47] fine-tuned the CNN to transfer knowledge. [167] proposed a siamese deep network of multi-task learning of FR and age estimation. [92] integrated feature extraction and metric learning via a deep CNN.

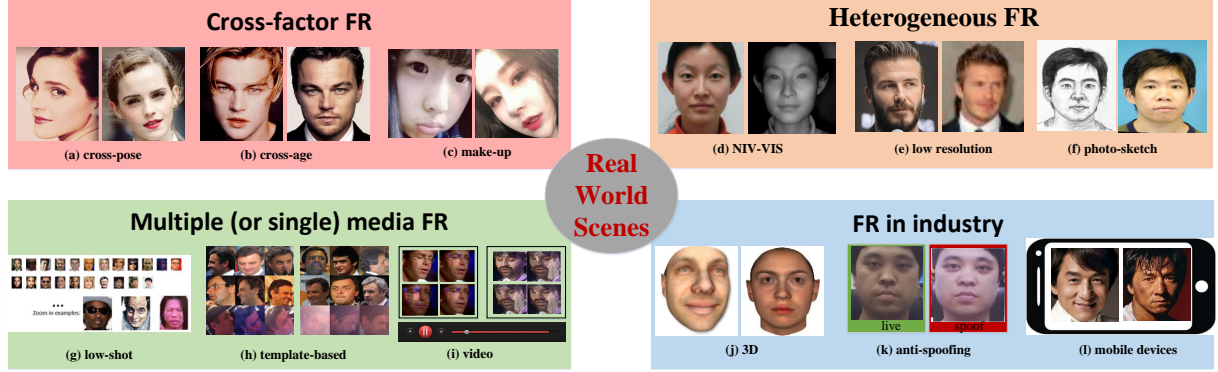


Fig. 13. The different scenes of FR.

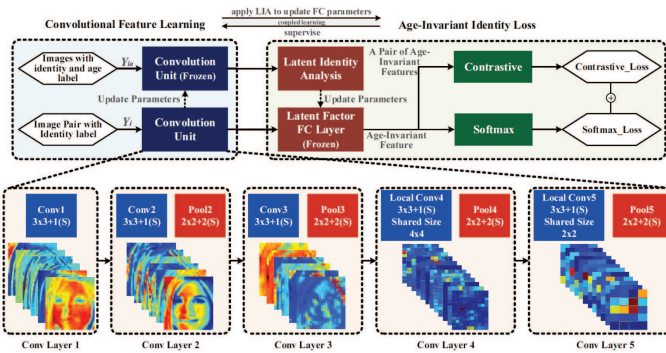


Fig. 14. The architecture of the cross-age FR with LIA. [169]

3) *Makeup Face Recognition*: Makeup is widely used by the public today, but it also brings challenges for FR due to significant facial appearance changes. The research on matching makeup and nonmakeup face images is receiving increasing attention. [91] generated nonmakeup images from makeup ones by a bi-level adversarial network (BLAN) and then used the synthesized nonmakeup images for verification. [145] pretrained a triplet network on the free videos and fine-tuned it on small makeup and nonmakeup datasets.

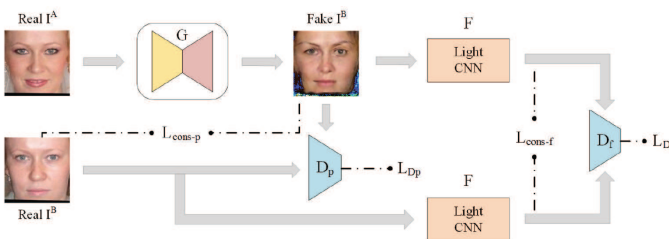


Fig. 15. The architecture of BLAN. [91]

B. Heterogenous Face Recognition

1) *NIR-VIS Face Recognition*: Due to the excellent performance of the near-infrared spectrum (NIS) images under low-light scenarios, NIS images are widely applied in surveillance systems. Because most enrolled databases consist of visible light (VIS) spectrum images, how to recognize a NIR face from a gallery of VIS images has been a hot topic. [133],

[100] transferred the VIS deep networks to the NIR domain by fine-tuning. [87] used a VIS CNN to recognize NIR faces by transforming NIR images to VIS faces through cross-spectral hallucination and restoring a low-rank structure for features through low-rank embedding. [125] trained two networks, a VISNet (for visible images) and a NIRNet (for near-infrared images), and coupled their output features by creating a siamese network. [62], [63] divided the high layer of the network into a NIR layer, a VIS layer and a NIR-VIS shared layer; then, a modality-invariant feature can be learned by the NIR-VIS shared layer. [142] embedded cross-spectral face hallucination and discriminative feature learning into an end-to-end adversarial network. In [177], the low-rank relevance and cross-modal ranking were used to alleviate the semantic gap.

2) *Low-Resolution Face Recognition*: Although deep networks are robust to a degree of low resolution, there are still a few studies focused on promoting the performance of low-resolution FR. For example, [198] proposed a CNN with a two-branch architecture (a super-resolution network and a feature extraction network) to map the high- and low-resolution face images into a common space where the intra-person distance is smaller than the inter-person distance.

3) *Photo-Sketch Face Recognition*: The photo-sketch FR may help law enforcement to quickly identify suspects. The commonly used methods can be categorized as two classes. One is to utilize transfer learning to directly match photos to sketches, where the deep networks are first trained using a large face database of photos and are then fine-tuned using small sketch database [106], [48]. The other is to use the image-to-image translation, where the photo can be transformed to a sketch or the sketch to a photo; then, FR can be performed in one domain. [201] developed a fully convolutional network with generative loss and a discriminative regularizer to transform photos to sketches. [199] utilized a branched fully convolutional neural network (BFCN) to generate a structure-preserved sketch and a texture-preserved sketch, and then they fused them together via a probabilistic method. Recently, GANs have achieved impressive results in image generation. [193], [83], [218] used two generators, G_A and G_B , to generate sketches from photos and photos from sketches, respectively. Based on [218], [163] proposed a

multi-adversarial network to avoid artifacts by leveraging the implicit presence of feature maps of different resolutions in the generator subnetwork.

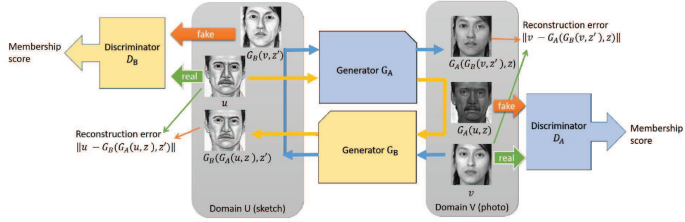


Fig. 16. The architecture of DualGAN. [193]

C. Multiple (or single) media Face Recognition

1) *Low-Shot Face Recognition*: For many practical applications, such as surveillance and security, the FR system should recognize persons with a very limited number of training samples or even with only one sample. The methods of low-shot learning can be categorized as enlarging the training data and learning more powerful features. [66] generated images in various poses using a 3D face model and adopted deep domain adaptation to handle the other variations, such as blur, occlusion, and expression. [29] used data augmentation methods and a GAN for pose transition and attribute boosting to increase the size of the training dataset. [178] proposed a framework with hybrid classifiers using a CNN and a nearest neighbor (NN) model. [55] made the norms of the weight vectors of the one-shot classes and the normal classes aligned to address the data imbalance problem. [27] proposed an enforced softmax that contains optimal dropout, selective attenuation, L2 normalization and model-level optimization.

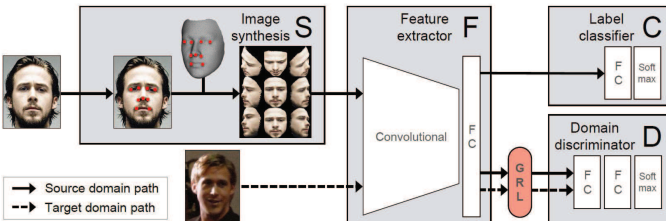


Fig. 17. The architecture of a single sample per person domain adaptation network (SSPP-DAN). [66]

2) *Set/Template-Based Face Recognition*: Set/template-based FR problems assume that both probe and gallery sets are represented using a set of media, e.g., images and videos, rather than just one. After learning a set of face representations from each medium individually, two strategies are generally adopted for face recognition between sets. One is to use these representations for similarity comparison between the media in two sets and pool the results into a single, final score, such as max score pooling [104], average score pooling [102] and its variations [210], [14]. The other strategy is to aggregate face representations through average or max pooling and generate a single representation for each set and then perform a comparison between two sets, which we call feature

pooling [104], [25], [130]. In addition to the commonly used strategies, there are also some novel methods proposed for set/template-based FR. For example, [59] proposed a deep heterogeneous feature fusion network to exploit the features' complementary information generated by different CNNs.

3) *Video Face Recognition*: There are two key issues in video FR: one is to integrate the information across different frames together to build a representation of the video face, and the other is to handle video frames with severe blur, pose variations, and occlusions. For frame aggregation, [190] proposed a neural aggregation network (NAN) in which the aggregation module, consisting of two attention blocks driven by a memory, produces a 128-dimensional vector representation. Rao et al. [123] aggregated raw video frames directly by combining the idea of metric learning and adversarial learning. For handling bad frames, [124] discarded the bad frames by treating this operation as a Markov decision process and trained the attention model through a deep reinforcement learning framework. [44] artificially blurred clear still images for training to learn blur-robust face representations. Parchami et al. [113] used a CNN to reconstruct a lower-quality video into a high-quality face.

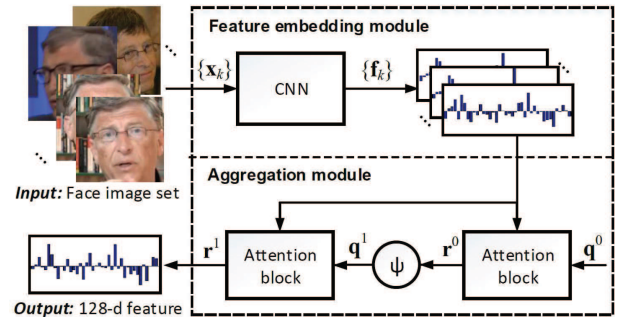


Fig. 18. The FR framework of NAN. [190]

D. Face Recognition in Industry

1) *3D Face Recognition*: 3D FR has inherent advantages over 2D methods, but 3D FR using deep networks is not well developed due to the lack of large annotated 3D data. To enlarge 3D training datasets, most works use the methods of “one-to-many augmentation” to synthesize 3D faces. However, the effective methods for extracting deep features of 3D faces remain to be explored. [81] fine-tuned a 2D CNN with a small amount of 3D scans for 3D FR. [223] used a three-channel (corresponding to depth, azimuth and elevation angles of the normal vector) image as input and minimized the average prediction log-loss. [200] selected 30 feature points from the Candide-3 face model to characterize faces and then conducted the unsupervised pretraining of face depth data and the supervised fine-tuning.

2) *Face Anti-spoofing*: With the success of FR techniques, various types of spoofing attacks, such as print attacks, replay attacks, and 3D mask attacks, are becoming a large threat. Face anti-spoofing is a very critical step to recognize whether the face is live or spoofed. Because it also needs to recognize faces (true or false identity), we treat it as one of the FR scenes. [7]

proposed a novel two-stream CNN in which the local features discriminate the spoof patches independent of the spatial face areas, and holistic depth maps ensure that the input live sample has a face-like depth. [188] trained a CNN using both a single frame and multiple frames with five scales, and the live/spoof label is assigned as the output. [185] proposed a long short-term memory (LSTM)-CNN architecture that learns temporal features to jointly predict for multiple frames of a video. [88], [116] fine-tuned their networks from a pretrained model by training sets of real and fake images.

3) *Face Recognition for Mobile Devices*: With the emergence of mobile phones, tablets and augmented reality, FR has been applied in mobile devices. Due to computational limitations, the recognition tasks in these devices need to be carried out in a light but timely fashion. As mentioned in Section III-C1, [73], [67], [30], [207] proposed lightweight deep networks, and these networks have potential to be introduced into FR. [150] proposed a multibatch method that first generates signatures for a minibatch of k face images and then constructs an unbiased estimate of the full gradient by relying on all $k^2 - k$ pairs from the minibatch.

V. CONCLUSIONS

In this paper, we provide a comprehensive survey of deep FR from two aspects of data and algorithms. For data, we summarize some commonly used FR datasets. Moreover, the methods of data preprocessing are introduced and categorized as “one-to-many augmentation” and “many-to-one normalization”. For algorithms, some typical and novel network architectures are presented. Meanwhile, we categorize loss functions into Euclidean-distance-based loss, angular/cosine-margin-based loss and softmax loss and its variations. Finally, the different scenes of deep FR, including video FR, 3D FR and cross-age FR, are briefly introduced.

Thanks to the massive amounts of annotated data, algorithms and GPUs, deep FR has achieved beyond human performance on some standard benchmarks on near-frontal face verification, similar-looking face discrimination, and cross-age face verification. However, comprehensive abilities are required before large-scale applications, and many issues still remain to be addressed, as follows:

- Because real-world FR is much more complex and strict than in the experiments, the FR system is still far from human performance in real-world settings. Improving the true positive rate while keeping a very low false positive rate is crucial; handling data bias and variations needs continued attention.
- Corresponding to three datasets, namely, MegaFace, MS-Celeb-1M and IJB-A, large-scale FR with a very large number of candidates, low/one-shot FR and large pose-variance FR will be the focus of research in the future.
- Face recognition can be inspired from human behaviors. For examples, for humans, familiar faces are recognized more accurately than unfamiliar ones and under difficult viewing conditions. Developing a deep model to encode face familiarity is important to FR under extreme conditions and open-set scenarios. Moreover, humans can

complete the recognition task in one step, so there is a bright prospect in the end-to-end system that jointly trains FR with several modules together.

- The first layer of deep networks can be viewed directly by visualization and is found to be similar to a Gabor filter, which realizes the edge detection. However, our understanding of how the whole deep networks operate, particularly what computations they perform at higher layers, has lagged behind. It is undoubtedly of great significance for the development of deep FR to open the black box and study the effective interpretation of high-level features.
- There are still many challenges in adopting deep FR in industry. Although face anti-spoofing has achieved successes in resisting print, replay, and 3D mask attacks, a new type of misclassification attack via physically realizable attack artifacts [138], [137] causes a rising interest, proving that FR systems are still not robust and are vulnerable to attacks. Meanwhile, the recognition tasks in mobile devices need to be carried out in a light but timely fashion. Therefore, improving the defensiveness of systems and the efficiency of computing are to be solved.
- Other challenges are included in our lists of deep FR scenes. When facing these different scenes in real-world settings, the system should make specific adjustments accordingly in order to achieve a very good effect. How to work out a more general system or a system that can be applied in every scene after little modification may be the direction in the future. Deep domain adaptation [164] has inherent advantages here and is worthy of attention.

REFERENCES

- [1] Fg-net aging database. <http://www.fgnet.rsunit.com>.
- [2] A. F. Abate, M. Nappi, D. Riccio, and G. Sabatino. 2d and 3d face recognition: A survey. *Pattern recognition letters*, 28(14):1885–1906, 2007.
- [3] W. Abdalmageed, Y. Wu, S. Rawls, S. Harel, T. Hassner, I. Masi, J. Choi, J. Lekust, J. Kim, and P. Natarajan. Face recognition using deep multi-pose representations. In *WACV*, pages 1–9, 2016.
- [4] T. Ahonen, A. Hadid, and M. Pietikainen. Face description with local binary patterns: Application to face recognition. *IEEE Trans. Pattern Anal. Machine Intell.*, 28(12):2037–2041, 2006.
- [5] G. Antipov, M. Baccouche, and J.-L. Dugelay. Boosting cross-age face verification via generative age normalization. In *IJCB*, 2017.
- [6] G. Antipov, M. Baccouche, and J.-L. Dugelay. Face aging with conditional generative adversarial networks. *arXiv preprint arXiv:1702.01983*, 2017.
- [7] Y. Atoum, Y. Liu, A. Jourabloo, and X. Liu. Face anti-spoofing using patch and depth-based cnns. In *IJCB*, pages 319–328. IEEE, 2017.
- [8] A. Bansal, C. Castillo, R. Ranjan, and R. Chellappa. The dos and donts for cnn-based face verification. *arXiv preprint arXiv:1705.07426*, 5, 2017.
- [9] A. Bansal, A. Nanduri, C. Castillo, R. Ranjan, and R. Chellappa. Umdfaces: An annotated face dataset for training deep networks. *arXiv preprint arXiv:1611.01484*, 2016.
- [10] P. N. Belhumeur, J. P. Hespanha, and D. J. Kriegman. Eigenfaces vs. fisherfaces: Recognition using class specific linear projection. *IEEE Trans. Pattern Anal. Mach. Intell.*, 19(7):711–720, 1997.
- [11] J. R. Beveridge, P. J. Phillips, D. S. Bolme, B. A. Draper, G. H. Givens, Y. M. Lui, M. N. Teli, H. Zhang, W. T. Scruggs, K. W. Bowyer, et al. The challenge of face recognition from digital point-and-shoot cameras. In *BTAS*, pages 1–8. IEEE, 2013.
- [12] S. Bianco. Large age-gap face verification by feature injection in deep networks. *Pattern Recognition Letters*, 90:36–42, 2017.
- [13] V. Blanz and T. Vetter. Face recognition based on fitting a 3d morphable model. *IEEE Transactions on pattern analysis and machine intelligence*, 25(9):1063–1074, 2003.

- [14] N. Bodla, J. Zheng, H. Xu, J.-C. Chen, C. Castillo, and R. Chellappa. Deep heterogeneous feature fusion for template-based face recognition. In *WACV*, pages 586–595. IEEE, 2017.
- [15] K. W. Bowyer, K. Chang, and P. Flynn. A survey of approaches and challenges in 3d and multi-modal 3d+ 2d face recognition. *Computer vision and image understanding*, 101(1):1–15, 2006.
- [16] K. Cao, Y. Rong, C. Li, X. Tang, and C. C. Loy. Pose-robust face recognition via deep residual equivariant mapping. *arXiv preprint arXiv:1803.00839*, 2018.
- [17] Q. Cao, L. Shen, W. Xie, O. M. Parkhi, and A. Zisserman. Vggface2: A dataset for recognising faces across pose and age. *arXiv preprint arXiv:1710.08092*, 2017.
- [18] Z. Cao, Q. Yin, X. Tang, and J. Sun. Face recognition with learning-based descriptor. In *CVPR*, pages 2707–2714. IEEE, 2010.
- [19] T.-H. Chan, K. Jia, S. Gao, J. Lu, Z. Zeng, and Y. Ma. Pcanet: A simple deep learning baseline for image classification? *IEEE Transactions on Image Processing*, 24(12):5017–5032, 2015.
- [20] B. Chen, W. Deng, and J. Du. Noisy softmax: improving the generalization ability of dcnn via postponing the early softmax saturation. *arXiv preprint arXiv:1708.03769*, 2017.
- [21] B.-C. Chen, C.-S. Chen, and W. H. Hsu. Cross-age reference coding for age-invariant face recognition and retrieval. In *ECCV*, pages 768–783. Springer, 2014.
- [22] D. Chen, X. Cao, L. Wang, F. Wen, and J. Sun. Bayesian face revisited: A joint formulation. In *ECCV*, pages 566–579. Springer, 2012.
- [23] D. Chen, X. Cao, F. Wen, and J. Sun. Blessing of dimensionality: High-dimensional feature and its efficient compression for face verification. In *CVPR*, pages 3025–3032, 2013.
- [24] G. Chen, Y. Shao, C. Tang, Z. Jin, and J. Zhang. Deep transformation learning for face recognition in the unconstrained scene. *Machine Vision and Applications*, pages 1–11, 2018.
- [25] J.-C. Chen, V. M. Patel, and R. Chellappa. Unconstrained face verification using deep cnn features. In *WACV*, pages 1–9. IEEE, 2016.
- [26] J.-C. Chen, R. Ranjan, A. Kumar, C.-H. Chen, V. M. Patel, and R. Chellappa. An end-to-end system for unconstrained face verification with deep convolutional neural networks. In *ICCV Workshops*, pages 118–126, 2015.
- [27] Y. Cheng, J. Zhao, Z. Wang, Y. Xu, K. Jayashree, S. Shen, and J. Feng. Know you at a glance: A compact vector representation for low-shot learning. In *CVPR*, pages 1924–1932, 2017.
- [28] I. Chingovska, A. Anjos, and S. Marcel. On the effectiveness of local binary patterns in face anti-spoofing, 2012.
- [29] J. Choe, S. Park, K. Kim, J. H. Park, D. Kim, and H. Shim. Face generation for low-shot learning using generative adversarial networks. In *ICCV Workshops*, pages 1940–1948. IEEE, 2017.
- [30] F. Chollet. Xception: Deep learning with depthwise separable convolutions. *arXiv preprint*, 2016.
- [31] A. R. Chowdhury, T.-Y. Lin, S. Maji, and E. Learned-Miller. One-to-many face recognition with bilinear cnns. In *WACV*, pages 1–9. IEEE, 2016.
- [32] F. Cole, D. Belanger, D. Krishnan, A. Sarna, I. Mosseri, and W. T. Freeman. Synthesizing normalized faces from facial identity features. In *CVPR*, pages 3386–3395, 2017.
- [33] N. Crosswhite, J. Byrne, C. Stauffer, O. Parkhi, Q. Cao, and A. Zisserman. Template adaptation for face verification and identification. In *FG 2017*, pages 1–8, 2017.
- [34] J. Deng, S. Cheng, N. Xue, Y. Zhou, and S. Zafeiriou. Uv-gan: Adversarial facial uv map completion for pose-invariant face recognition. *arXiv preprint arXiv:1712.04695*, 2017.
- [35] J. Deng, J. Guo, and S. Zafeiriou. Arcface: Additive angular margin loss for deep face recognition. *arXiv preprint arXiv:1801.07698*, 2018.
- [36] J. Deng, Y. Zhou, and S. Zafeiriou. Marginal loss for deep face recognition. In *CVPR Workshops*, volume 4, 2017.
- [37] W. Deng, J. Hu, and J. Guo. Extended src: Undersampled face recognition via intraclass variant dictionary. *IEEE Trans. Pattern Anal. Machine Intell.*, 34(9):1864–1870, 2012.
- [38] W. Deng, J. Hu, and J. Guo. Compressive binary patterns: Designing a robust binary face descriptor with random-field eigenfilters. *IEEE Trans. Pattern Anal. Mach. Intell.*, PP(99):1–1, 2018.
- [39] W. Deng, J. Hu, and J. Guo. Face recognition via collaborative representation: Its discriminant nature and superposed representation. *IEEE Trans. Pattern Anal. Mach. Intell.*, PP(99):1–1, 2018.
- [40] W. Deng, J. Hu, J. Guo, H. Zhang, and C. Zhang. Comments on “globally maximizing, locally minimizing: Unsupervised discriminant projection with applications to face and palm biometrics”. *IEEE Trans. Pattern Anal. Mach. Intell.*, 30(8):1503–1504, 2008.
- [41] W. Deng, J. Hu, J. Lu, and J. Guo. Transform-invariant pca: A unified approach to fully automatic facealignment, representation, and recognition. *IEEE Trans. Pattern Anal. Mach. Intell.*, 36(6):1275–1284, June 2014.
- [42] W. Deng, J. Hu, N. Zhang, B. Chen, and J. Guo. Fine-grained face verification: Fglfw database, baselines, and human-dcmn partnership. *Pattern Recognition*, 66:63–73, 2017.
- [43] C. Ding and D. Tao. Robust face recognition via multimodal deep face representation. *IEEE Transactions on Multimedia*, 17(11):2049–2058, 2015.
- [44] C. Ding and D. Tao. Trunk-branch ensemble convolutional neural networks for video-based face recognition. *IEEE transactions on pattern analysis and machine intelligence*, 2017.
- [45] P. Dou, S. K. Shah, and I. A. Kakadiaris. End-to-end 3d face reconstruction with deep neural networks. In *CVPR*, volume 5, 2017.
- [46] C. N. Duong, K. G. Quach, K. Luu, M. Savvides, et al. Temporal non-volume preserving approach to facial age-progression and age-invariant face recognition. *arXiv preprint arXiv:1703.08617*, 2017.
- [47] H. El Khiyari and H. Wechsler. Age invariant face recognition using convolutional neural networks and set distances. *Journal of Information Security*, 8(03):174, 2017.
- [48] C. Galea and R. A. Farrugia. Forensic face photo-sketch recognition using a deep learning-based architecture. *IEEE Signal Processing Letters*, 24(11):1586–1590, 2017.
- [49] M. M. Ghazi and H. K. Ekenel. A comprehensive analysis of deep learning based representation for face recognition. In *CVPR Workshops*, volume 26, pages 34–41, 2016.
- [50] I. Goodfellow, J. Pouget-Abadie, M. Mirza, B. Xu, D. Warde-Farley, S. Ozair, A. Courville, and Y. Bengio. Generative adversarial nets. In *NIPS*, pages 2672–2680, 2014.
- [51] P. J. Grother and L. N. Mei. Face recognition vendor test (frvt) performance of face identification algorithms nist ir 8009. *NIST Interagency/Internal Report (NISTIR) - 8009*, 2014.
- [52] G. Guo, L. Wen, and S. Yan. Face authentication with makeup changes. *IEEE Transactions on Circuits and Systems for Video Technology*, 24(5):814–825, 2014.
- [53] S. Guo, S. Chen, and Y. Li. Face recognition based on convolutional neural network and support vector machine. In *IEEE International Conference on Information and Automation*, pages 1787–1792, 2017.
- [54] Y. Guo, J. Zhang, J. Cai, B. Jiang, and J. Zheng. 3dfacenet: Real-time dense face reconstruction via synthesizing photo-realistic face images. 2017.
- [55] Y. Guo and L. Zhang. One-shot face recognition by promoting underrepresented classes. *arXiv preprint arXiv:1707.05574*, 2017.
- [56] Y. Guo, L. Zhang, Y. Hu, X. He, and J. Gao. Ms-celeb-1m: A dataset and benchmark for large-scale face recognition. In *ECCV*, pages 87–102. Springer, 2016.
- [57] A. Hasnat, J. Bohné, J. Milgram, S. Gentric, and L. Chen. Deepvisage: Making face recognition simple yet with powerful generalization skills. *arXiv preprint arXiv:1703.08388*, 2017.
- [58] M. Hasnat, J. Bohné, J. Milgram, S. Gentric, L. Chen, et al. von mises-fisher mixture model-based deep learning: Application to face verification. *arXiv preprint arXiv:1706.04264*, 2017.
- [59] M. Hayat, M. Bennamoun, and S. An. Learning non-linear reconstruction models for image set classification. In *CVPR*, pages 1907–1914, 2014.
- [60] M. Hayat, S. H. Khan, N. Werghi, and R. Goecke. Joint registration and representation learning for unconstrained face identification. In *CVPR*, pages 2767–2776, 2017.
- [61] K. He, X. Zhang, S. Ren, and J. Sun. Deep residual learning for image recognition. In *CVPR*, pages 770–778, 2016.
- [62] R. He, X. Wu, Z. Sun, and T. Tan. Learning invariant deep representation for nir-vis face recognition. In *AAAI*, volume 4, page 7, 2017.
- [63] R. He, X. Wu, Z. Sun, and T. Tan. Wasserstein cnn: Learning invariant features for nir-vis face recognition. *arXiv preprint arXiv:1708.02412*, 2017.
- [64] X. He, S. Yan, Y. Hu, P. Niyogi, and H.-J. Zhang. Face recognition using laplacianfaces. *IEEE Trans. Pattern Anal. Mach. Intell.*, 27(3):328–340, 2005.
- [65] G. E. Hinton, S. Osindero, and Y.-W. Teh. A fast learning algorithm for deep belief nets. *Neural computation*, 18(7):1527–1554, 2006.
- [66] S. Hong, W. Im, J. Ryu, and H. S. Yang. Sppp-dan: Deep domain adaptation network for face recognition with single sample per person. *arXiv preprint arXiv:1702.04069*, 2017.
- [67] A. G. Howard, M. Zhu, B. Chen, D. Kalenichenko, W. Wang, T. Weyand, M. Andreetto, and H. Adam. Mobilenets: Efficient convolutional neural networks for mobile vision applications. *arXiv preprint arXiv:1704.04861*, 2017.
- [68] G. Hu, Y. Yang, D. Yi, J. Kittler, W. Christmas, S. Z. Li, and T. Hospedales. When face recognition meets with deep learning: an evaluation of convolutional neural networks for face recognition. In *ICCV workshops*, pages 142–150, 2015.
- [69] J. Hu, Y. Ge, J. Lu, and X. Feng. Makeup-robust face verification. In *ICASSP*, pages 2342–2346. IEEE, 2013.

- [70] L. Hu, M. Kan, S. Shan, X. Song, and X. Chen. Ldf-net: Learning a displacement field network for face recognition across pose. In *FG 2017*, pages 9–16. IEEE, 2017.
- [71] G. B. Huang, M. Ramesh, T. Berg, and E. Learned-Miller. Labeled faces in the wild: A database for studying face recognition in unconstrained environments. Technical report, Technical Report 07-49, University of Massachusetts, Amherst, 2007.
- [72] R. Huang, S. Zhang, T. Li, R. He, et al. Beyond face rotation: Global and local perception gan for photorealistic and identity preserving frontal view synthesis. *arXiv preprint arXiv:1704.04086*, 2017.
- [73] F. N. Iandola, S. Han, M. W. Moskewicz, K. Ashraf, W. J. Dally, and K. Keutzer. SqueezeNet: Alexnet-level accuracy with 50x fewer parameters and; 0.5 mb model size. *arXiv preprint arXiv:1602.07360*, 2016.
- [74] M. Jaderberg, K. Simonyan, A. Zisserman, et al. Spatial transformer networks. In *NIPS*, pages 2017–2025, 2015.
- [75] R. Jafri and H. R. Arabnia. A survey of face recognition techniques. *Jips*, 5(2):41–68, 2009.
- [76] H. Jegou, M. Douze, and C. Schmid. Product quantization for nearest neighbor search. *IEEE Transactions on Pattern Analysis & Machine Intelligence*, 33(1):117, 2011.
- [77] M. Kan, S. Shan, H. Chang, and X. Chen. Stacked progressive auto-encoders (spae) for face recognition across poses. In *CVPR*, pages 1883–1890, 2014.
- [78] M. Kan, S. Shan, and X. Chen. Bi-shifting auto-encoder for unsupervised domain adaptation. In *ICCV*, pages 3846–3854, 2015.
- [79] M. Kan, S. Shan, and X. Chen. Multi-view deep network for cross-view classification. In *CVPR*, pages 4847–4855, 2016.
- [80] I. Kemelmacher-Shlizerman, S. M. Seitz, D. Miller, and E. Brossard. The megaface benchmark: 1 million faces for recognition at scale. In *CVPR*, pages 4873–4882, 2016.
- [81] D. Kim, M. Hernandez, J. Choi, and G. Medioni. Deep 3d face identification. *arXiv preprint arXiv:1703.10714*, 2017.
- [82] M. Kim, S. Kumar, V. Pavlovic, and H. Rowley. Face tracking and recognition with visual constraints in real-world videos. In *CVPR*, pages 1–8. IEEE, 2008.
- [83] T. Kim, M. Cha, H. Kim, J. Lee, and J. Kim. Learning to discover cross-domain relations with generative adversarial networks. *arXiv preprint arXiv:1703.05192*, 2017.
- [84] B. F. Klare, B. Klein, E. Taborsky, A. Blanton, J. Cheney, K. Allen, P. Grother, A. Mah, and A. K. Jain. Pushing the frontiers of unconstrained face detection and recognition: Iarpa janus benchmark a. In *CVPR*, pages 1931–1939, 2015.
- [85] A. Krizhevsky, I. Sutskever, and G. E. Hinton. Imagenet classification with deep convolutional neural networks. In *NIPS*, pages 1097–1105, 2012.
- [86] Z. Lei, M. Pietikainen, and S. Z. Li. Learning discriminant face descriptor. *IEEE Trans. Pattern Anal. Machine Intell.*, 36(2):289–302, 2014.
- [87] J. Lezama, Q. Qiu, and G. Sapiro. Not afraid of the dark: Nir-vis face recognition via cross-spectral hallucination and low-rank embedding. In *CVPR*, pages 6807–6816. IEEE, 2017.
- [88] L. Li, X. Feng, Z. Boulkenafet, Z. Xia, M. Li, and A. Hadid. An original face anti-spoofing approach using partial convolutional neural network. In *IPTA*, pages 1–6. IEEE, 2016.
- [89] S. Z. Li, D. Yi, Z. Lei, and S. Liao. The casia nir-vis 2.0 face database. In *CVPR workshops*, pages 348–353. IEEE, 2013.
- [90] S. Z. Li, L. Zhen, and A. Meng. The hfb face database for heterogeneous face biometrics research. In *CVPR Workshops*, pages 1–8, 2009.
- [91] Y. Li, L. Song, X. Wu, R. He, and T. Tan. Anti-makeup: Learning a bi-level adversarial network for makeup-invariant face verification. *arXiv preprint arXiv:1709.03654*, 2017.
- [92] Y. Li, G. Wang, L. Nie, Q. Wang, and W. Tan. Distance metric optimization driven convolutional neural network for age invariant face recognition. *Pattern Recognition*, 75:51–62, 2018.
- [93] L. Lin, G. Wang, W. Zuo, X. Feng, and L. Zhang. Cross-domain visual matching via generalized similarity measure and feature learning. *IEEE Transactions on Pattern Analysis & Machine Intelligence*, 39(6):1089–1102, 2016.
- [94] T.-Y. Lin, A. RoyChowdhury, and S. Maji. Bilinear cnn models for fine-grained visual recognition. In *ICCV*, pages 1449–1457, 2015.
- [95] C. Liu and H. Wechsler. Gabor feature based classification using the enhanced fisher linear discriminant model for face recognition. *Image processing, IEEE Transactions on*, 11(4):467–476, 2002.
- [96] J. Liu, Y. Deng, T. Bai, Z. Wei, and C. Huang. Targeting ultimate accuracy: Face recognition via deep embedding. *arXiv preprint arXiv:1506.07310*, 2015.
- [97] W. Liu, Y. Wen, Z. Yu, M. Li, B. Raj, and L. Song. Sphereface: Deep hypersphere embedding for face recognition. In *CVPR*, volume 1, 2017.
- [98] W. Liu, Y. Wen, Z. Yu, and M. Yang. Large-margin softmax loss for convolutional neural networks. In *ICML*, pages 507–516, 2016.
- [99] W. Liu, Y.-M. Zhang, X. Li, Z. Yu, B. Dai, T. Zhao, and L. Song. Deep hyperspherical learning. In *NIPS*, pages 3953–3963, 2017.
- [100] X. Liu, L. Song, X. Wu, and T. Tan. Transferring deep representation for nir-vis heterogeneous face recognition. In *ICB*, pages 1–8. IEEE, 2016.
- [101] Y. Liu, H. Li, and X. Wang. Rethinking feature discrimination and polymerization for large-scale recognition. *arXiv preprint arXiv:1710.00870*, 2017.
- [102] J. Lu, G. Wang, W. Deng, P. Moulin, and J. Zhou. Multi-manifold deep metric learning for image set classification. In *CVPR*, pages 1137–1145, 2015.
- [103] I. Masi, T. Hassner, A. T. Tran, and G. Medioni. Rapid synthesis of massive face sets for improved face recognition. In *FG 2017*, pages 604–611. IEEE, 2017.
- [104] I. Masi, S. Rawls, G. Medioni, and P. Natarajan. Pose-aware face recognition in the wild. In *CVPR*, pages 4838–4846, 2016.
- [105] I. Masi, A. T. Tr?n, T. Hassner, J. T. Leksut, and G. Medioni. Do we really need to collect millions of faces for effective face recognition? In *ECCV*, pages 579–596. Springer, 2016.
- [106] P. Mittal, M. Vatsa, and R. Singh. Composite sketch recognition via deep network-a transfer learning approach. In *ICB*, pages 251–256. IEEE, 2015.
- [107] B. Moghaddam, W. Wahid, and A. Pentland. Beyond eigenfaces: probabilistic matching for face recognition. *Automatic Face and Gesture Recognition, 1998. Proc. Third IEEE Int. Conf.*, pages 30–35, Apr 1998.
- [108] A. Nech and I. Kemelmacher-Shlizerman. Level playing field for million scale face recognition. In *CVPR*, pages 3406–3415. IEEE, 2017.
- [109] H.-W. Ng and S. Winkler. A data-driven approach to cleaning large face datasets. In *ICIP*, pages 343–347. IEEE, 2014.
- [110] S. Ouyang, T. Hospedales, Y.-Z. Song, X. Li, C. C. Loy, and X. Wang. A survey on heterogeneous face recognition: Sketch, infra-red, 3d and low-resolution. *Image and Vision Computing*, 56:28–48, 2016.
- [111] S. J. Pan and Q. Yang. A survey on transfer learning. *IEEE Transactions on knowledge and data engineering*, 22(10):1345–1359, 2010.
- [112] G. Panis, A. Lanitis, N. Tsapatsoulis, and T. F. Cootes. Overview of research on facial ageing using the fg-net ageing database. *IET Biometrics*, 5(2):37–46, 2016.
- [113] M. Parchami, S. Bashbaghi, E. Granger, and S. Sayed. Using deep autoencoders to learn robust domain-invariant representations for still-to-video face recognition. In *AVSS*, pages 1–6. IEEE, 2017.
- [114] C. J. Parde, C. Castillo, M. Q. Hill, Y. I. Colon, S. Sankaranarayanan, J.-C. Chen, and A. J. O’Toole. Deep convolutional neural network features and the original image. *arXiv preprint arXiv:1611.01751*, 2016.
- [115] O. M. Parkhi, A. Vedaldi, A. Zisserman, et al. Deep face recognition. In *BMVC*, volume 1, page 6, 2015.
- [116] K. Patel, H. Han, and A. K. Jain. Cross-database face antispoofing with robust feature representation. In *Chinese Conference on Biometric Recognition*, pages 611–619. Springer, 2016.
- [117] X. Peng, X. Yu, K. Sohn, D. N. Metaxas, and M. Chandraker. Reconstruction-based disentanglement for pose-invariant face recognition. *intervals*, 20:12, 2017.
- [118] P. J. Phillips, P. J. Flynn, T. Scruggs, K. W. Bowyer, J. Chang, K. Hoffman, J. Marques, J. Min, and W. Worek. Overview of the face recognition grand challenge. In *CVPR*, volume 1, pages 947–954. IEEE, 2005.
- [119] X. Qi and L. Zhang. Face recognition via centralized coordinate learning. *arXiv preprint arXiv:1801.05678*, 2018.
- [120] R. Ranjan, C. D. Castillo, and R. Chellappa. L2-constrained softmax loss for discriminative face verification. *arXiv preprint arXiv:1703.09507*, 2017.
- [121] R. Ranjan, S. Sankaranarayanan, A. Bansal, N. Bodla, J. C. Chen, V. M. Patel, C. D. Castillo, and R. Chellappa. Deep learning for understanding faces: Machines may be just as good, or better, than humans. *IEEE Signal Processing Magazine*, 35(1):66–83, 2018.
- [122] R. Ranjan, S. Sankaranarayanan, C. D. Castillo, and R. Chellappa. An all-in-one convolutional neural network for face analysis. In *FG 2017*, pages 17–24. IEEE, 2017.
- [123] Y. Rao, J. Lin, J. Lu, and J. Zhou. Learning discriminative aggregation network for video-based face recognition. In *CVPR*, pages 3781–3790, 2017.
- [124] Y. Rao, J. Lu, and J. Zhou. Attention-aware deep reinforcement learning for video face recognition. In *CVPR*, pages 3931–3940, 2017.
- [125] C. Reale, N. M. Nasrabadi, H. Kwon, and R. Chellappa. Seeing the forest from the trees: A holistic approach to near-infrared heteroge-

- neous face recognition. In *CVPR Workshops*, pages 320–328. IEEE, 2016.
- [126] K. Ricanek and T. Tesafaye. Morph: A longitudinal image database of normal adult age-progressions. In *FGR*, pages 341–345. IEEE, 2006.
- [127] E. Richardson, M. Sela, and R. Kimmel. 3d face reconstruction by learning from synthetic data. In *3DV*, pages 460–469. IEEE, 2016.
- [128] E. Richardson, M. Sela, R. Or-El, and R. Kimmel. Learning detailed face reconstruction from a single image. In *CVPR*, pages 5553–5562. IEEE, 2017.
- [129] O. Russakovsky, J. Deng, H. Su, J. Krause, S. Satheesh, S. Ma, Z. Huang, A. Karpathy, A. Khosla, M. Bernstein, et al. Imagenet large scale visual recognition challenge. *International Journal of Computer Vision*, 115(3):211–252, 2015.
- [130] S. Sankaranarayanan, A. Alavi, C. D. Castillo, and R. Chellappa. Triplet probabilistic embedding for face verification and clustering. In *BTAS*, pages 1–8. IEEE, 2016.
- [131] S. Sankaranarayanan, A. Alavi, and R. Chellappa. Triplet similarity embedding for face verification. *arXiv preprint arXiv:1602.03418*, 2016.
- [132] A. Savran, N. Alyüz, H. Dibeklioğlu, O. Çeliktutan, B. Gökberk, B. Sankur, and L. Akarun. Bosphorus database for 3d face analysis. In *European Workshop on Biometrics and Identity Management*, pages 47–56. Springer, 2008.
- [133] S. Saxena and J. Verbeek. Heterogeneous face recognition with cnns. In *ECCV*, pages 483–491. Springer, 2016.
- [134] A. Scheenstra, A. Ruifrok, and R. C. Veltkamp. A survey of 3d face recognition methods. In *International Conference on Audio-and Video-based Biometric Person Authentication*, pages 891–899. Springer, 2005.
- [135] F. Schroff, D. Kalenichenko, and J. Philbin. Facenet: A unified embedding for face recognition and clustering. In *CVPR*, pages 815–823, 2015.
- [136] S. Sengupta, J.-C. Chen, C. Castillo, V. M. Patel, R. Chellappa, and D. W. Jacobs. Frontal to profile face verification in the wild. In *WACV*, pages 1–9. IEEE, 2016.
- [137] M. Sharif, S. Bhagavatula, L. Bauer, and M. K. Reiter. Accessorize to a crime: Real and stealthy attacks on state-of-the-art face recognition. In *Proceedings of the 2016 ACM SIGSAC Conference on Computer and Communications Security*, pages 1528–1540. ACM, 2016.
- [138] M. Sharif, S. Bhagavatula, L. Bauer, and M. K. Reiter. Adversarial generative nets: Neural network attacks on state-of-the-art face recognition. *arXiv preprint arXiv:1801.00349*, 2017.
- [139] A. Shrivastava, T. Pfister, O. Tuzel, J. Susskind, W. Wang, and R. Webb. Learning from simulated and unsupervised images through adversarial training. In *CVPR*, volume 3, page 6, 2017.
- [140] K. Simonyan and A. Zisserman. Very deep convolutional networks for large-scale image recognition. *arXiv preprint arXiv:1409.1556*, 2014.
- [141] K. Sohn, S. Liu, G. Zhong, X. Yu, M.-H. Yang, and M. Chandraker. Unsupervised domain adaptation for face recognition in unlabeled videos. *arXiv preprint arXiv:1708.02191*, 2017.
- [142] L. Song, M. Zhang, X. Wu, and R. He. Adversarial discriminative heterogeneous face recognition. *arXiv preprint arXiv:1709.03675*, 2017.
- [143] Y. Sun, Y. Chen, X. Wang, and X. Tang. Deep learning face representation by joint identification-verification. In *NIPS*, pages 1988–1996, 2014.
- [144] Y. Sun, D. Liang, X. Wang, and X. Tang. Deepid3: Face recognition with very deep neural networks. *arXiv preprint arXiv:1502.00873*, 2015.
- [145] Y. Sun, L. Ren, Z. Wei, B. Liu, Y. Zhai, and S. Liu. A weakly supervised method for makeup-invariant face verification. *Pattern Recognition*, 66:153–159, 2017.
- [146] Y. Sun, X. Wang, and X. Tang. Hybrid deep learning for face verification. In *ICCV*, pages 1489–1496. IEEE, 2013.
- [147] Y. Sun, X. Wang, and X. Tang. Deep learning face representation from predicting 10,000 classes. In *CVPR*, pages 1891–1898, 2014.
- [148] Y. Sun, X. Wang, and X. Tang. Sparsifying neural network connections for face recognition. In *CVPR*, pages 4856–4864, 2016.
- [149] C. Szegedy, W. Liu, Y. Jia, P. Sermanet, S. Reed, D. Anguelov, D. Erhan, V. Vanhoucke, A. Rabinovich, et al. Going deeper with convolutions. *Cvpr*, 2015.
- [150] O. Tadmor, Y. Wexler, T. Rosenwein, S. Shalev-Shwartz, and A. Shamir. Learning a metric embedding for face recognition using the multibatch method. *arXiv preprint arXiv:1605.07270*, 2016.
- [151] Y. Taigman, M. Yang, M. Ranzato, and L. Wolf. Deepface: Closing the gap to human-level performance in face verification. In *CVPR*, pages 1701–1708, 2014.
- [152] A. Tewari, M. Zollhöfer, H. Kim, P. Garrido, F. Bernard, P. Perez, and C. Theobalt. MoFa: Model-based deep convolutional face autoencoder for unsupervised monocular reconstruction. In *ICCV*, volume 2, 2017.
- [153] A. T. Tran, T. Hassner, I. Masi, and G. Medioni. Regressing robust and discriminative 3d morphable models with a very deep neural network. In *CVPR*, pages 1493–1502. IEEE, 2017.
- [154] L. Tran, X. Yin, and X. Liu. Disentangled representation learning gan for pose-invariant face recognition. In *CVPR*, volume 3, page 7, 2017.
- [155] M. Turk and A. Pentland. Eigenfaces for recognition. *Journal of cognitive neuroscience*, 3(1):71–86, 1991.
- [156] E. Tzeng, J. Hoffman, K. Saenko, and T. Darrell. Adversarial discriminative domain adaptation. In *CVPR*, volume 1, page 4, 2017.
- [157] P. Vincent, H. Larochelle, I. Lajoie, Y. Bengio, and P.-A. Manzagol. Stacked denoising autoencoders: Learning useful representations in a deep network with a local denoising criterion. *Journal of Machine Learning Research*, 11(Dec):3371–3408, 2010.
- [158] D. Wang, C. Otto, and A. K. Jain. Face search at scale: 80 million gallery. *arXiv preprint arXiv:1507.07242*, 2015.
- [159] D. Wang, C. Otto, and A. K. Jain. Face search at scale. *IEEE transactions on pattern analysis and machine intelligence*, 39(6):1122–1136, 2017.
- [160] F. Wang, W. Liu, H. Liu, and J. Cheng. Additive margin softmax for face verification. *arXiv preprint arXiv:1801.05599*, 2018.
- [161] F. Wang, X. Xiang, J. Cheng, and A. L. Yuille. Normface: l_2 hypersphere embedding for face verification. *arXiv preprint arXiv:1704.06369*, 2017.
- [162] H. Wang, Y. Wang, Z. Zhou, X. Ji, Z. Li, D. Gong, J. Zhou, and W. Liu. Cosface: Large margin cosine loss for deep face recognition. *arXiv preprint arXiv:1801.09414*, 2018.
- [163] L. Wang, V. A. Sindagi, and V. M. Patel. High-quality facial photo-sketch synthesis using multi-adversarial networks. *arXiv preprint arXiv:1710.10182*, 2017.
- [164] M. Wang and W. Deng. Deep visual domain adaptation: A survey. *arXiv preprint arXiv:1802.03601*, 2018.
- [165] W. Wang, Z. Cui, H. Chang, S. Shan, and X. Chen. Deeply coupled auto-encoder networks for cross-view classification. *arXiv preprint arXiv:1402.2031*, 2014.
- [166] X. Wang and X. Tang. Face photo-sketch synthesis and recognition. *IEEE Transactions on Pattern Analysis and Machine Intelligence*, 31(11):1955–1967, 2009.
- [167] X. Wang, Y. Zhou, D. Kong, J. Currey, D. Li, and J. Zhou. Unleash the black magic in age: a multi-task deep neural network approach for cross-age face verification. In *FG 2017*, pages 596–603. IEEE, 2017.
- [168] K. Q. Weinberger and L. K. Saul. Distance metric learning for large margin nearest neighbor classification. *Journal of Machine Learning Research*, 10(Feb):207–244, 2009.
- [169] Y. Wen, Z. Li, and Y. Qiao. Latent factor guided convolutional neural networks for age-invariant face recognition. In *CVPR*, pages 4893–4901, 2016.
- [170] Y. Wen, K. Zhang, Z. Li, and Y. Qiao. A discriminative feature learning approach for deep face recognition. In *ECCV*, pages 499–515. Springer, 2016.
- [171] L. Wolf, T. Hassner, and I. Maoz. Face recognition in unconstrained videos with matched background similarity. In *CVPR*, pages 529–534. IEEE, 2011.
- [172] J. Wright, A. Yang, A. Ganesh, S. Sastry, and Y. Ma. Robust Face Recognition via Sparse Representation. *IEEE Trans. Pattern Anal. Machine Intell.*, 31(2):210–227, 2009.
- [173] W.-S. T. WST. Deeply learned face representations are sparse, selective, and robust. *perception*, 31:411–438, 2008.
- [174] W. Wu, M. Kan, X. Liu, Y. Yang, S. Shan, and X. Chen. Recursive spatial transformer (rest) for alignment-free face recognition. In *CVPR*, pages 3772–3780, 2017.
- [175] X. Wu, R. He, and Z. Sun. A lightened cnn for deep face representation. In *CVPR*, volume 4, 2015.
- [176] X. Wu, R. He, Z. Sun, and T. Tan. A light cnn for deep face representation with noisy labels. *arXiv preprint arXiv:1511.02683*, 2015.
- [177] X. Wu, L. Song, R. He, and T. Tan. Coupled deep learning for heterogeneous face recognition. *arXiv preprint arXiv:1704.02450*, 2017.
- [178] Y. Wu, H. Liu, and Y. Fu. Low-shot face recognition with hybrid classifiers. In *CVPR*, pages 1933–1939, 2017.
- [179] Y. Wu, H. Liu, J. Li, and Y. Fu. Deep face recognition with center invariant loss. In *Proceedings of the on Thematic Workshops of ACM Multimedia 2017*, pages 408–414. ACM, 2017.
- [180] S. Xie and Z. Tu. Holistically-nested edge detection. In *ICCV*, pages 1395–1403, 2015.
- [181] E. P. Xing, M. I. Jordan, S. J. Russell, and A. Y. Ng. Distance metric learning with application to clustering with side-information. In *NIPS*, pages 521–528, 2003.
- [182] C. Xiong, X. Zhao, D. Tang, K. Jayashree, S. Yan, and T.-K. Kim. Conditional convolutional neural network for modality-aware face recognition. In *ICCV*, pages 3667–3675. IEEE, 2015.

- [183] L. Xiong, J. Karlekar, J. Zhao, J. Feng, S. Pranata, and S. Shen. A good practice towards top performance of face recognition: Transferred deep feature fusion. *arXiv preprint arXiv:1704.00438*, 2017.
- [184] Y. Xu, S. Shen, J. Feng, J. Xing, Y. Cheng, J. Zhao, Z. Wang, L. Xiong, K. Jayashree, and H. Tamura. High performance large scale face recognition with multi-cognition softmax and feature retrieval. In *ICCV Workshop*, pages 1898–1906, 2017.
- [185] Z. Xu, S. Li, and W. Deng. Learning temporal features using lstm-cnn architecture for face anti-spoofing. In *ACPR*, pages 141–145. IEEE, 2015.
- [186] S. Yan, D. Xu, B. Zhang, and H.-J. Zhang. Graph embedding: A general framework for dimensionality reduction. *Computer Vision and Pattern Recognition, IEEE Computer Society Conference on*, 2:830–837, 2005.
- [187] H. Yang and I. Patras. Mirror, mirror on the wall, tell me, is the error small? In *CVPR*, pages 4685–4693, 2015.
- [188] J. Yang, Z. Lei, and S. Z. Li. Learn convolutional neural network for face anti-spoofing. *arXiv preprint arXiv:1408.5601*, 2014.
- [189] J. Yang, S. E. Reed, M.-H. Yang, and H. Lee. Weakly-supervised disentangling with recurrent transformations for 3d view synthesis. In *NIPS*, pages 1099–1107, 2015.
- [190] J. Yang, P. Ren, D. Chen, F. Wen, H. Li, and G. Hua. Neural aggregation network for video face recognition. *arXiv preprint arXiv:1603.05474*, 2016.
- [191] M. Yang, X. Wang, G. Zeng, and L. Shen. Joint and collaborative representation with local adaptive convolution feature for face recognition with single sample per person. *Pattern Recognition*, 66(C):117–128, 2016.
- [192] D. Yi, Z. Lei, S. Liao, and S. Z. Li. Learning face representation from scratch. *arXiv preprint arXiv:1411.7923*, 2014.
- [193] Z. Yi, H. Zhang, P. Tan, and M. Gong. Dualgan: Unsupervised dual learning for image-to-image translation. *arXiv preprint*, 2017.
- [194] J. Yim, H. Jung, B. Yoo, C. Choi, D. Park, and J. Kim. Rotating your face using multi-task deep neural network. In *CVPR*, pages 676–684, 2015.
- [195] L. Yin, X. Wei, Y. Sun, J. Wang, and M. J. Rosato. A 3d facial expression database for facial behavior research. In *FGR*, pages 211–216. IEEE, 2006.
- [196] X. Yin and X. Liu. Multi-task convolutional neural network for pose-invariant face recognition. *TIP*, 2017.
- [197] X. Yin, X. Yu, K. Sohn, X. Liu, and M. Chandraker. Towards large-pose face frontalization in the wild. *arXiv preprint arXiv:1704.06244*, 2017.
- [198] E. Zangeneh, M. Rahmati, and Y. Mohsenzadeh. Low resolution face recognition using a two-branch deep convolutional neural network architecture. *arXiv preprint arXiv:1706.06247*, 2017.
- [199] D. Zhang, L. Lin, T. Chen, X. Wu, W. Tan, and E. Izquierdo. Content-adaptive sketch portrait generation by decompositional representation learning. *IEEE Transactions on Image Processing*, 26(1):328–339, 2017.
- [200] J. Zhang, Z. Hou, Z. Wu, Y. Chen, and W. Li. Research of 3d face recognition algorithm based on deep learning stacked denoising autoencoder theory. In *ICCSN*, pages 663–667. IEEE, 2016.
- [201] L. Zhang, L. Lin, X. Wu, S. Ding, and L. Zhang. End-to-end photo-sketch generation via fully convolutional representation learning. In *Proceedings of the 5th ACM on International Conference on Multimedia Retrieval*, pages 627–634. ACM, 2015.
- [202] L. Zhang, M. Yang, and X. Feng. Sparse representation or collaborative representation: Which helps face recognition? In *ICCV*, 2011.
- [203] W. Zhang, S. Shan, W. Gao, X. Chen, and H. Zhang. Local gabor binary pattern histogram sequence (lgbphs): A novel non-statistical model for face representation and recognition. In *ICCV*, volume 1, pages 786–791. IEEE, 2005.
- [204] W. Zhang, X. Wang, and X. Tang. Coupled information-theoretic encoding for face photo-sketch recognition. In *CVPR*, pages 513–520. IEEE, 2011.
- [205] X. Zhang, Z. Fang, Y. Wen, Z. Li, and Y. Qiao. Range loss for deep face recognition with long-tail. *arXiv preprint arXiv:1611.08976*, 2016.
- [206] X. Zhang and Y. Gao. Face recognition across pose: A review. *Pattern Recognition*, 42(11):2876–2896, 2009.
- [207] X. Zhang, X. Zhou, M. Lin, and J. Sun. Shufflenet: An extremely efficient convolutional neural network for mobile devices. *arXiv preprint arXiv:1707.01083*, 2017.
- [208] Y. Zhang, M. Shao, E. K. Wong, and Y. Fu. Random faces guided sparse many-to-one encoder for pose-invariant face recognition. In *ICCV*, pages 2416–2423. IEEE, 2013.
- [209] Z. Zhang, J. Yan, S. Liu, Z. Lei, D. Yi, and S. Z. Li. A face antispoofing database with diverse attacks. In *ICB*, pages 26–31, 2012.
- [210] J. Zhao, J. Han, and L. Shao. Unconstrained face recognition using a set-to-set distance measure on deep learned features. *IEEE Transactions on Circuits and Systems for Video Technology*, 2017.
- [211] J. Zhao, L. Xiong, P. K. Jayashree, J. Li, F. Zhao, Z. Wang, P. S. Pranata, P. S. Shen, S. Yan, and J. Feng. Dual-agent gans for photorealistic and identity preserving profile face synthesis. In *NIPS*, pages 65–75, 2017.
- [212] W. Zhao, R. Chellappa, P. J. Phillips, and A. Rosenfeld. Face recognition: A literature survey. *ACM computing surveys (CSUR)*, 35(4):399–458, 2003.
- [213] T. Zheng and W. Deng. Cross-pose lfw: A database for studying cross-pose face recognition in unconstrained environments. Technical Report 18-01, Beijing University of Posts and Telecommunications, February 2018.
- [214] T. Zheng, W. Deng, and J. Hu. Age estimation guided convolutional neural network for age-invariant face recognition. In *CVPR Workshops*, pages 1–9, 2017.
- [215] T. Zheng, W. Deng, and J. Hu. Cross-age lfw: A database for studying cross-age face recognition in unconstrained environments. *arXiv preprint arXiv:1708.08197*, 2017.
- [216] Y. Zhong, J. Chen, and B. Huang. Toward end-to-end face recognition through alignment learning. *IEEE signal processing letters*, 24(8):1213–1217, 2017.
- [217] E. Zhou, Z. Cao, and Q. Yin. Naive-deep face recognition: Touching the limit of lfw benchmark or not? *arXiv preprint arXiv:1501.04690*, 2015.
- [218] J.-Y. Zhu, T. Park, P. Isola, and A. A. Efros. Unpaired image-to-image translation using cycle-consistent adversarial networks. *arXiv preprint arXiv:1703.10593*, 2017.
- [219] Z. Zhu, P. Luo, X. Wang, and X. Tang. Deep learning identity-preserving face space. In *ICCV*, pages 113–120. IEEE, 2013.
- [220] Z. Zhu, P. Luo, X. Wang, and X. Tang. Multi-view perceptron: a deep model for learning face identity and view representations. In *NIPS*, pages 217–225, 2014.
- [221] Z. Zhu, P. Luo, X. Wang, and X. Tang. Recover canonical-view faces in the wild with deep neural networks. *arXiv preprint arXiv:1404.3543*, 2014.
- [222] X. Zou, J. Kittler, and K. Messer. Illumination invariant face recognition: A survey. In *BTAS*, pages 1–8. IEEE, 2007.
- [223] S. Zulqarnain Gilani and A. Mian. Learning from millions of 3d scans for large-scale 3d face recognition. *arXiv preprint arXiv:1711.05942*, 2017.